A Hillslope Hydrology Analysis of the Landscape Evolution Observatory within Biosphere 2

Bachelor's thesis – definitive version

UNIVERSITY OF TWENTE.

THE UNIVERSITY OF ARIZONA®

Daniël van den Heuvel

University of Twente

University of Arizona

06/30/2016

A Hillslope Hydrology Analysis of the Landscape Evolution Observatory within Biosphere 2

Author:
Daniël van den Heuvel
Bachelor's student Civil Engineering
Faculty of Engineering Technology
University of Twente, the Netherlands

Supervisor home university
Dr. ir. M.J. Booij
Associate professor
Faculty of Engineering Technology
Department of Water Engineering and Management

External supervisor
Dr. P.A. Troch
Professor
Department of Hydrology and Water Resources
University of Arizona, USA

Internship carried out from April 18th through July 1st 2016.

Preface

This thesis marks the end of the internship I conducted at the department of Hydrology and Water Resources at the University of Arizona in Tucson, USA. During my time in Tucson I have experienced countless new adventures and gotten to know numerous friendly Americans whom I could share a laugh with when I was not working on this thesis. They have most certainly contributed to making this internship abroad an experience to never forget. This report also marks the end of my time as a Bachelor's student at the University of Twente, a time during which I have learnt about countless subjects related to civil engineering, developed a tremendous number of academic skills and during which I have gotten to know many good friends.

Furthermore, I would like to take this opportunity to thank several people who have been very helpful before, during and after my stay in the USA. In the first place I would like to thank Martijn Booij, for putting me in touch with Peter Troch and supervising me during the entire process of writing a research proposal and the actual thesis. I greatly appreciated his elaborate and sharp-cut feedback on various matters which certainly helped me improve this thesis. Of course, I also thank Peter Troch whole-heartedly for giving me the opportunity to conduct this research in his department and his helpful remarks regarding the content of this thesis. It was an honor and a pleasure to make a contribution to one of the most advanced and scientifically acclaimed projects in this particular field of research.

Additionally, I would like to express my gratitude to Ellen van Oosterzee and Erma Santander, who helped me through the time-demanding and complex procedure of obtaining a J-1 visa for the USA. I finally render thanks to various staff members at the University of Arizona and Biosphere 2 for supporting me in any way they could, in particular Guo-Yue Niu for his assistance and patience with regard to the hydrological model CATHY. Neither this research project itself nor the practicalities around my stay in Tucson could have taken off without the help these people have provided.

Daniël van den Heuvel
Tucson, AZ, USA
June 30th, 2016

Summary

The Landscape Evolution Observatory (LEO) is a modern and multidisciplinary research project aiming to shed light on the role that coupled processes play in landscape evolution. These processes are generally attributed to the disciplines of (a) hydrology, (b) ecology, (c) geochemistry and (d) geomorphology. The LEO project comprises three identical artificial hillslopes upon which artificial precipitation may be cast in an endeavor to improve understanding of these coupled processes' nature and relations. The hillslopes sit in a fully controlled environment, overcoming the barrier of unknown boundary conditions and internal structures that field experiments tend to encounter.

Previous experiments at LEO have revealed that water transit times are significantly longer in the western slope than in the central slope. In turn, preliminary analysis of the results has led the scientists to believe that the central and east slopes' responses are more resemblant. Considering that the hillslopes were designed to be fully identical in shape, technical equipment and soil characteristics, this difference should not exist. This research aims to identify what differences between the central and west slopes may have brought about the glaring discrepancy in the two slopes' responses to rainfall-runoff experiments.

A thorough analysis of data that was previously gathered shows that water transit times are indeed significantly longer in the west slope, because of its tendency to discharge water more slowly. Since the slopes' geometry and technical equipment had previously been found to be similar, the research's focal point was shifted to the soil characteristics. Examination of newly plotted soil water retention curves fitted to the Van Genuchten model reveals considerable variation in the fitting parameters α^{-1} and n. It was therefore decided to concentrate on differences among these two parameters and the soil's saturated hydraulic conductivity, K_s, which partially depends on n.

Through simulations of the central and west hillslope using already known east slope input parameters in the hydrological model CATchment HYdrology (CATHY), this thesis illustrates that the central and east slopes bear less resemblance than was previously assumed. In fact, this simulation shows that the west slope is more similar to the east slope than the central slope. Subsequently, the three parameters are calibrated for both slopes using CATHY as part of this research. To do so, about 1,200 simulations have been generated with CATHY under randomized values for α^{-1}, n and K_s within certain ranges. These ranges were inspired by analysis of the various soil water retention curves which had been plotted. The twenty parameter combinations which yielded the best goodness-of-fit as compared with observed data are then compared in both cases.

From these results the conclusion is drawn that mainly the parameter α^{-1} exhibits a sharp distinction between both hillslopes, indicating a difference in the depth of the slopes' capillary fringe. The value of α^{-1} was found to be in the order of –0.2 m in the central slope and approximately –0.45 m in the west slope. The Van Genuchten model suggests that greater absolute values of α^{-1} enhance water retention characteristics, thus explaining why the west slope discharges water more slowly than its centrally located counterpart. While values of n and K_s did show slight variation between the two slopes, these differences are deemed too small to be accountable for the substantial discrepancy in responses as was observed.

It was impossible to make conclusive claims as to why exactly the depth of the capillary fringe appears to differ in both hillslopes. However, the hypothesis that the west slope contains more fine soil particles than the central slope has been formulated, explaining why the west slope discharges more slowly despite its similar soil porosity. It is suggested that this hypothesis be tested in further research to deliver conclusive proof with regard to the found physical difference among both slopes.

Table of contents

List of figures and tables

1 Introduction

This introductory chapter first provides the reader with details about the scientific context in which this research has taken place. The state of the art is discussed in detail in section 1.2. From this state of the art, the research gap of this study is distilled afterward. Subsequently, the aim of this research is specified in section 1.4, along with several research questions which help establish a clear structure throughout this thesis. Finally, section 1.5 serves as a thesis outline, which aims to familiarize the reader with this thesis' structure in the upcoming chapters.

1.1 Scientific context

Over the past few decades, many studies in hillslope hydrology have focused on modeling rainfall-runoff processes and the great extent of heterogeneity and complexity that comes with them (McDonnell et al., 2007). Hydrologists have made various attempts to apply models to different watersheds, in different climates and to different scales. However, in spite of this myriad of attempts, their models often did not resemble experimental data gathered.

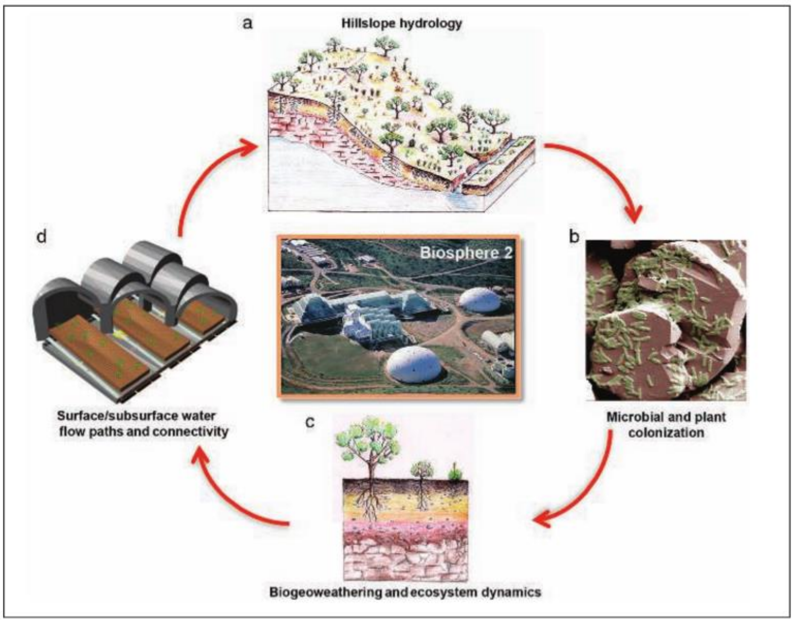

Figure 1: The four key processes playing a major role in landscape evolution: (a) hydrology, (b) ecology, (c) geochemistry and (d) geomorphology. Reprinted from "The Hills are Alive: Earth Science in a Controlled Environment" by T.E. Huxman, 2009, *Eos Transactions American Geophysical Union*, p. 1.

Recently, numerous studies have advocated a new theory for hillslope hydrology, which should include a better understanding of the coupled nature of many different processes involved in landscape evolution (Hopp et al., 2009; Lin et al., 2006; Wagener et al, 2007). These natural processes are generally associated with (a) hydrology, (b) ecology, (c) geochemistry and (d) geomorphology, though variations exist. The interdependent relations of these processes are depicted in Figure 1 (Huxman et al., 2009). Although the interactivity of these processes is well-known and their influence on landscape evolution is widely acknowledged, it remains difficult to conduct reliable field experiments to prove this (Dontsova et al., 2009; Pangle et al., 2015). Due to unknown boundary conditions and internal system structures, field experiments are often reduced to sampling for approximations of model parameters (Eberhardt & Thomas, 1991; McDonnell et al., 2007).

In order to overcome this hurdle and be able to understand the various coupled processes, the University of Arizona broke ground in 2007 on a massive interdisciplinary research project, which would be dubbed Landscape Evolution Observatory, hereafter: LEO. The project's goal is to understand the system of different interactive natural processes and its influence on the formation of landscapes over time. This knowledge can then be used to shed light on past landscape changes and predict future landscape evolution. LEO should therefore be considered a research tool enabling scientists to improve their understanding of coupled processes in watersheds and to make educated predictions of future landscape changes.

Other projects aimed at elucidating coupled hydrologic processes have been initiated in the past. For instance, an artificial water catchment (“Chicken Creek”) was constructed nearby Lusatia in Germany (Gerwin et al., 2009; Hofer et al., 2011). This project has enabled local researchers to define boundaries and internal structures at watershed level before conducting experiments. This has helped them better understand the various processes that play a role and implicates that the watershed is no longer a black box because of unknown internal structures.

Another significant research project revolving around hillslope hydrology and other related disciplines is the Terrestrial Environmental Observatories (TERENO) program (Bogena et al., 2016; Zacharias et al., 2011). Its goal is to observe long-term effects of climate change and global change on terrestrial systems, which extend from the nearby subsurface to the lower atmosphere. This research project entails a network of observatories in Germany and focuses on observing and understanding the effects that climate change may have on this region in the world. All observatories are at watershed scale and are closely monitored, but important conditions such as precipitation and temperature are not controlled.

Although these extensive research projects have some parallels with LEO, there are some considerable differences as well. While the German projects focus on watershed areas of around 10,000 km^2 in area, LEO takes place at a whole other scale, comprising only three artificial hillslopes. Not only does LEO sit in a completely controlled environment, allowing researchers to modify important conditions such as temperature and humidity, it is also equipped with cutting-edge measurement technology to monitor a variety of parameters at a high resolution in space and time. This makes LEO unique in its field.

In a broader context, the LEO project serves to understand and predict the impact that climate change may have on water resources and ecosystems. Although climate change is often associated with tremendous water surpluses due to globally rising temperatures and resulting excess meltwater from arctic regions, arid regions face severe risks as well. The southwestern parts of the United States have, for instance, started to become drier and will probably continue to dry out over the next decades (Seager et al., 2007). Since these particular areas are especially prone to increasing aridity, it is logical that many hydrological and environmental research departments focusing on drought problems are situated here. This is also the case for LEO, which is part of the Biosphere 2 complex in Oracle, near Tucson, Arizona.

1.2 State of the art

Construction of LEO within Biosphere 2 was finished in 2012. The result consists of three artificial hillslopes measuring approximately 30 meters in length by 11.15 meters in width. The average slope is about 10° and is convergent. Figure 2 visualizes the slopes' geometry (Hopp et al., 2009). Crushed basalt rock was used as a homogeneous soil layer of 1 meter thickness. Moreover, the three hillslopes are built identically in both shape and soil properties. The landscapes sit in a controlled environment with over 1,700 sensors and samplers per hillslope, so that important quantities of water, carbon and energy cycling processes can be measured. For example, soil water content, temperature and CO_2-

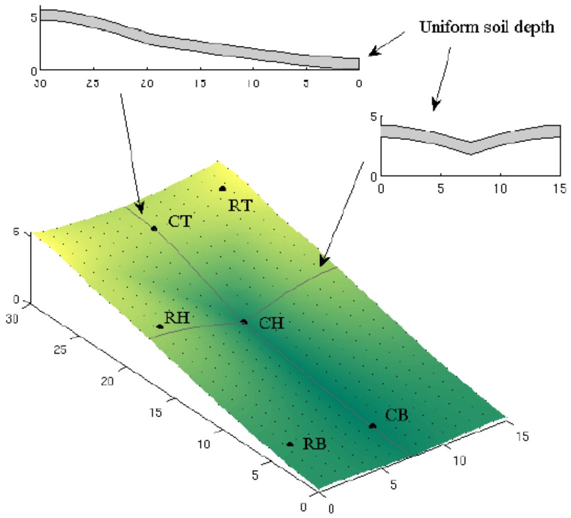

Figure 2: Basic geometry for the three convergent hillslopes, which measure 30 x 11.15 meters. Note that the slopes' width in the actually constructed LEO is 11.15 meters rather than the 15 meters shown here. Reprinted from “Hillslope hydrology under glass: confronting fundamental questions of soil-water-biota co-evolution at Biosphere 2” by L. Hopp et al., 2009, *Hydrology and Earth System Sciences*, p. 2109.

concentrations can be monitored continuously. Also, artificial precipitation can be cast upon the hillslopes, varying from 4 to 48 mm/h. As of yet, there is no vegetation at all on the hillslopes, as the researchers want to focus on the bare hillslope properties first. When these properties are sufficiently understood, vegetation will be added so that the model advances to a higher realism level and thus a higher complexity level.

In addition to conducting experiments on the physical hillslope model, researchers have attempted to build a computational model capable of predicting water flows within LEO. The governing model that is used in the project is named CATHY (CATchment HYdrology), sometimes coupled with NOAH-MP (NOAH-Multiple Processes). CATHY is a 3D subsurface hydrology model and NOAH-MP is a land surface model (LSM) (Camporese et al., 2010). This coupling allows for the simulation of water flows below and above the hillslope surfaces. Both models have been calibrated for LEO's east slope specifically. The ultimate goal is to build a model which can predict real-life landscape evolution using many input parameters. In essence the calibrated CATHY and NOAH-MP are models of a model: water flows within the LEO hill slopes are modeled using both computational models and LEO is a model of a possible real-life watershed. For the remainder of this thesis the physical model and computational model must be clearly distinguished. The former entails the physical experimental set-up of the three hillslopes, the latter the calibrated coupling of CATHY and NOAH-MP. Because this research solely focuses on subsurface flows, CATHY is the governing model in this research.

Until now, the focal point of experiments at LEO has mainly been the hydrologic properties of the hillslopes. More specifically, their water transit times, capability of generating subsurface flows and transport flows of fine soil particles and isotope tracers have been investigated. During the first experiment, the east hillslope was brought into a steady state through long-lasting precipitation on the slope. It was then discovered that measurements of water transit times through the slopes and flow characteristics differed significantly from model predictions. In fact, overland flow occurred whereas it was predicted that all the water would infiltrate through seepage. This prompted the researchers to alter their model parameters so that computer model predictions would be in accordance measurements. Overall, the east slope has been studied and modeled using CATHY the most. The latest script of CATHY for LEO specifically was therefore calibrated using east slope results (Niu et al., 2014).

During later experiments it was discovered that the rainfall-runoff response is quite different for the two other hillslopes. The west and central slopes were tested almost simultaneously, but their response differed considerably. More specifically, the west slope appeared to retain water longer than the central slope. This means that it takes more time for precipitation cast upon the west slope to be discharged. It is important to note that both slopes' runoff coefficients are both in the order of 68% and do not differ much. So, at an identical precipitation time and intensity, both slopes eventually discharge approximately the same amount of water. This means the average discharge/precipitation ratio is similar for both slopes. This discharge process is slower for the west slope, so that its discharge-over-time curve is flatter than for its central counterpart. Precipitation was cast on the east slope in a separate event and preliminary analysis showed an outcome closer to the central slope's response. However, because the experiment on the east slope was conducted at a different point in time and under different circumstances, this research focuses on the central and west slopes. The fact that these two slopes appear to respond rather differently is concerning, as the slopes are supposed to be fully identical in shape, soil composition and measurement techniques.

Although no definitive answer to this question has been found yet, researchers at Biosphere 2 have reasons to believe that two soil parameters are mainly responsible for the differences, being the hydraulic conductivity and the water retention characteristic. Unlike many other parameters (such as the slopes' dimensions, precipitation rates, temperature and soil material) these parameters have not yet been proven to be alike for the two slopes. As stated before, vegetation cannot play a role because there is none yet.

1.3 Research gap

The state of the art described in the previous section reveals a research gap that currently exists in the LEO project at Biosphere 2. It would appear that for a reason yet to be understood the west slope's physical rainfall-runoff response within LEO differs significantly from the central slope's response, since the west slope appears to retain the same amount of water for a longer period. The central slope thus discharges faster than the west slope, although their runoff coefficients are about the same. In other words, there is a discrepancy between the water transit times of both slopes, but not between the total amount of water eventually discharged. The reason for this difference, which should not exist as the slopes, measuring equipment and precipitation are assumed to be identical, makes up the research gap.

1.4 Research aim

The aim of this research project is to find out why the west slope retains water from artificial precipitation much longer than its centrally located counterpart within Biosphere 2 in spite of their seemingly identicalness in geometry, soil composition, measuring equipment and artificial precipitation. This is achieved by analyzing previously collected data and fitting theoretical soil water retention curves according to the Van Genuchten model to the observed data. Additionally, the hydrological model CATHY is used to generate many simulations of the experiments conducted on the slopes under different soil characteristics in order to estimate the optimal soil characteristics which best simulate observations made. The optimal soil characteristics are eventually compared in order to conclude whether soil water retention characteristics do actually differ. The following research questions are formulated to pave the way in closing the research gap:

"How significantly – in hydrological terms – do water transit times in the physical central and west LEO hillslopes differ from each other?" ***(1)***

"Which properties of the two hillslopes have not yet been confirmed to be alike and could thus be responsible for differences in water transit times between the central and west hillslopes?" ***(2)***

"How reliably can the central and west slopes' responses be simulated in CATHY using east slope input parameters and is it justifiable to use east slope input parameters to simulate one of them?" ***(3)***

"How do the analyzed model parameters differ for the central and west slope cases and can they explain the observed discrepancy between water transit times in both slopes?" ***(4)***

"How do the central and west slopes in Biosphere 2 physically differ from each other with respect to the analyzed parameters?" ***(5)***

Research question (5) is attuned to the previously formulated research aim. It aims to close the research gap stated before. Research question (1) mainly focuses on further specifying the problem and assessing its size. Along with questions (2) and (3) it should be thought of as means to find the answer to question (4). To answer these three questions, some auxiliary tools in the form of data, literature, experts and CATHY are available. The result of question (4) should pave the way to answer question (5) and thus help close the research gap. This structure is visualized in Figure 3.

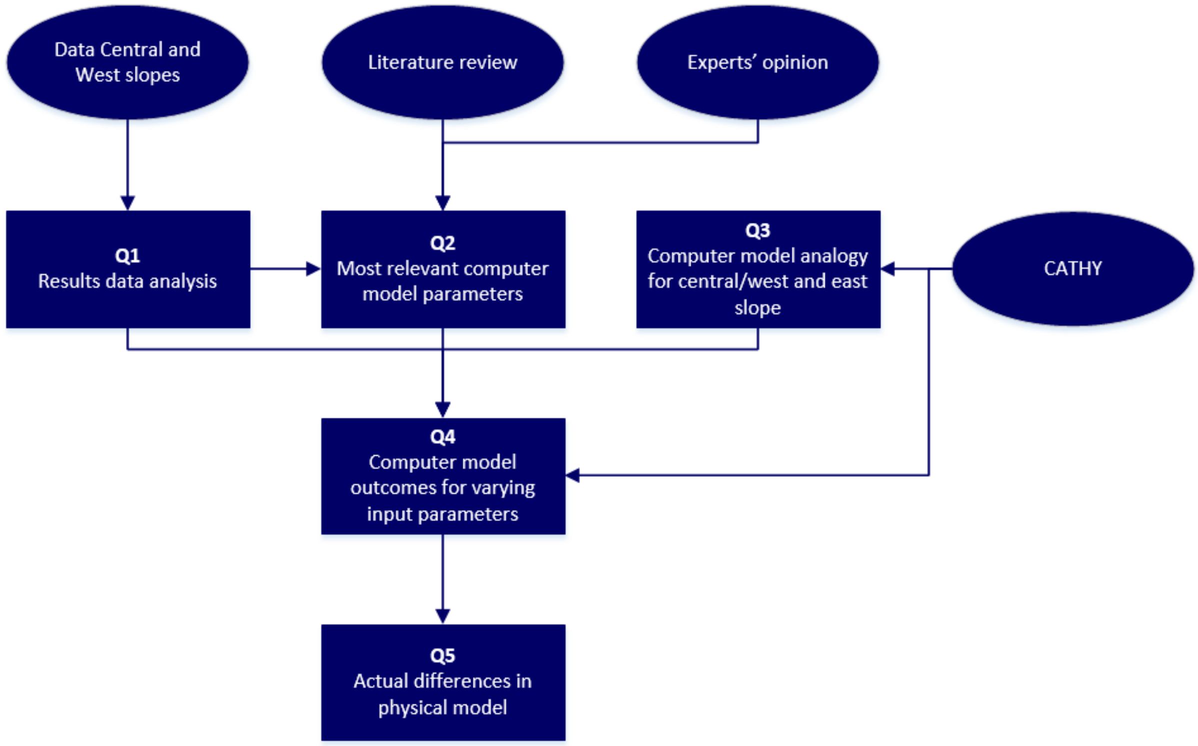

Figure 3: Overview of all research questions and auxiliary tools and their mutual relations.

1.5 Thesis outline

The remainder of this thesis maintains the following structure. Chapter 2 goes into details on the properties of the LEO hillslopes, the manner in which they were erected and to what extent their properties are identical. Additionally, it describes the way vital data is collected from the hillslopes and present the characteristics of the various data sets used.

The purpose of chapter 3 is to provide the reader with some necessary background knowledge of the governing computer model, CATHY and its role in this research.

Chapter 4 illustrates the methodology employed to answer the research questions that were formulated earlier. Each section in that chapter corresponds to one research question (for example, section 4.2 clarifies which method was applied to find the answer to research question 2).

Results are first reported in chapter 5, along with a detailed analysis of these results and partial conclusions based on them. Again, this chapter's structure corresponds to the structure employed in chapter 4, providing the reader with the convenience to easily review the methodology utilized to answer a particular research question.

The results described are subject to discussion in chapter 6, where a critical stance toward this research is taken to review its methodologies and results. Finally, chapter 7 includes conclusions for all research questions and formulates an answer referring back to the initial research aim. In addition, some recommendations for further research are given based on the outcomes of this project.

2 Physical model and data acquisition

This chapter serves to describe the experimental set-up, hillslope characteristics and measurement techniques at LEO research grounds. First, the hillslope characteristics are thoroughly outlined in section 2.1, so that the central and west slopes' properties become clear. Afterward, the measurement techniques and used data sets are subject to description.

2.1 Physical model characteristics

This section elucidates several aspects of both the central and west slopes in LEO, such as the slopes' geometry, soil composition, artificial precipitation equipment, seepage face and some key hydrological concepts related to soil.

2.1.1 Geometry

The three slopes' geometry was previously confirmed to be identical. The slopes all measure 30 m x 11.15 m, so that their two-dimensional area is 334.5 m^2 (Niu et al., 2014). Moreover, their slope over the 30 meter course is identical at about 10° on average. All slopes work with their own coordinate system, of which an example can found to the right, in Figure 4 (Pangle et al., 2015). All experimental equipment can be localized using this coordinate system. Figure 4 also shows the slopes' convergent nature. Additionally, each slope is categorized into five layers. These layers are, measured from the soil surface, localized at –0.05 m, –0.2 m, –0.35 m, –0.5 m and –0.85 m soil depth and are respectively designated with layer 1 through 5.

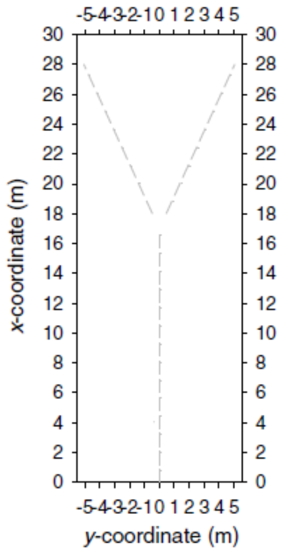

Figure 4: Basic 2D geometry and coordinate system for each hillslope. Adapted from "The Landscape Evolution Observatory: A large-scale controllable infrastructure to study coupled Earth-surface processes" by L.A. Pangle et al., 2015, *Geomorphology,* p. 196.

2.1.2 Soil composition

The bare steel structures forming the foundation of the three hillslopes were filled with crushed basaltic tephra ground, which falls into the texture category of loamy sand. There were various reasons to use basalt as the hillslope soil in LEO, most importantly because of its favorable hydraulic properties allowing sufficient storage for vegetation to eventually grow on the slopes. Crucial to this research was that the basalt's hydraulic conductivity was not too high, preventing formation of local heterogeneity (Pangle et al., 2015).

However, one study did report soil in the east slope might have become heterogeneous upon a heavy rainfall experiment (Niu et al., 2014). It concluded that the overland flow occurring in the experiment, which was not predicted by computer model simulations prior to the actual experiment, was probably due to transport of fine soil particles in the downstream direction. Similar results using the same soil type had previously been found under laboratory conditions (Hernandez & Schaap, 2012). Fine particles may have accumulated at the seepage face of the slope and caused the hydraulic conductivity to be locally lower, rendering the hillslope soil with heterogeneous characteristics. Since no overland flow was reported during previous experiments on the central and west slopes, this study assumes homogeneous soil properties across both hillslopes, meaning that the saturated hydraulic conductivity is considered equal throughout the slopes.

The 334.5 m^2 steel structures underlying the LEO hillslopes were filled with 334.5 m^3 of crushed basalt, so that a uniform and initially homogeneous layer of approximately 1 m would form the artificial hillslopes. The soil depth was measured in subsequent studies. Figure 5 visualizes the soil depth of the west (left), central (middle) and east (right) slopes. Although all slopes eventually appeared to have soil layers exceeding 1.0 m in depth, the west slope visibly contains the most basalt material (Pangle et al., 2015).

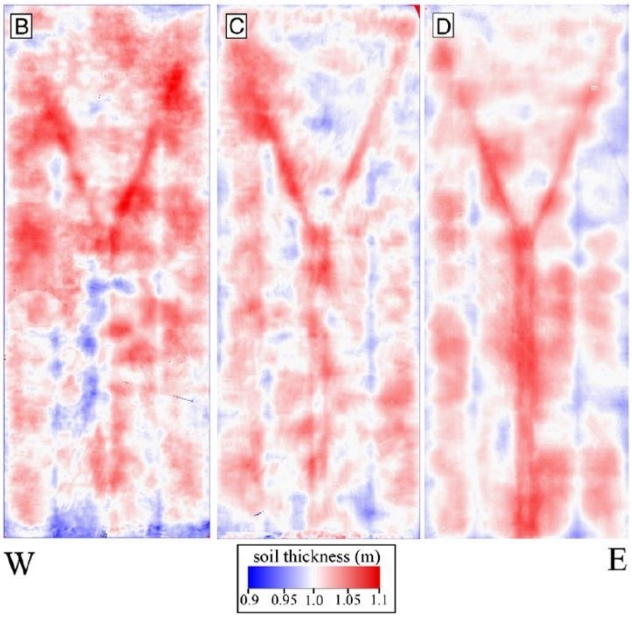

Figure 5: Local soil depths variation in the west (left), central (middle) and east (right) hillslopes within LEO. Soil depths were derived from laser scans before and after soil was applied to the underlying steel structures. Adapted from "The Landscape Evolution Observatory: A large-scale controllable infrastructure to study coupled Earth-surface processes" by L.A. Pangle et al., 2015, *Geomorphology*, p. 194.

2.1.3 Precipitation

Artificial precipitation can be cast on the hillslopes using 14 sprinkler heads installed above each slope. These sprinklers are spaced out equally, sit approximately 3 meters above soil surface and are capable of a total precipitation rate of 48 mm h^{-1} when all circuits operate at maximum capacity (Pangle et al., 2015).

2.1.4 Seepage face

The lower boundary of each hillslope system is located at the lower end of the slope. At this boundary, the soil is immediately adjacent to a layer of basaltic tephra with gravel structure measuring 0.5 m upslope-length (Pangle et al., 2015). This boundary layer of gravel is abutted by a perforated plastic sheet with tiny holes with a 2 mm diameter at its lower end. Steel supports and beams divide the seepage face into six different sections, each of which has its own discharge measurements (see section 2.2.1).

2.1.5 Water balance

The water balance is a pivotal equation used to describe flows of water going in and out of a system and the resulting change in water storage in that system. Adding up and subtracting flows leads to the change in water storage over time of the system. The water balance for each LEO hillslope can be written as follows:

$$\Delta S = P - E - Q \quad [1]$$

where ΔS is the change in water storage [L T^{-1}], P the precipitation falling on the hillslope [L T^{-1}], E the evaporation [L T^{-1}] and Q the discharge of water from the system through the seepage face [L T^{-1}]. The water balance shows that there is only one way for water to get into the system and two ways to leave it. Note that E was used rather than the more common ET for evapotranspiration, since the lack of vegetation on the slopes implies the absence of transpiration.

The water storage, precipitation and discharge rates can all be derived from data gathered from each hillslope. Although E is not measured directly, it may be found from the water balance as all other parameters are known: $E = P - \Delta S - Q$.

2.1.6 Saturated hydraulic conductivity

The hydraulic conductivity is usually denoted by K and represents the facility with which fluids can move through a porous medium, in this case LEO's soil. Because research at LEO focuses on water flows through the hillslope soil during and after precipitation has been cast on the soil, it is logical to use the soil's hydraulic conductivity under saturated conditions, K_s.

There exists a variety in models describing the relations between the soil's (saturated) hydraulic conductivity and the volumetric water content. Previous studies on LEO's east slope (Hazenberg et al., 2016; Niu et al., 2014) used the Mualem model for this (Mualem, 1976). This model is therefore assumed in this research as well:

$$K_h(\theta) = K_{h,s} S_e^{\lambda} (1 - (1 - S_e^{\frac{n}{n-1}})^{\frac{n-1}{n}})^2 \quad [2]$$

where θ is the volumetric water content [$L^3\ L^{-3}$], $S_e = (\theta - \theta_r / \theta_s - \theta_r)$ [–], θ_r is the residual volumetric water content [$L^3\ L^{-3}$], θ_s is the saturated volumetric water content (equal to the porosity) [$L^3\ L^{-3}$], λ is a fitting parameter (usually constant at 0.5) [–] and n is a representation of the pore size distribution [–].

2.1.7 Soil water retention characteristic

Each soil type has its own characteristic with regard to its ability to retain water. For example, it is well known that clay is less permeable and retains more water than a sandy soil. This characteristic is usually visualized in a soil water retention curve, some examples of which can be found in Figure 6 (Tuller & Or, 2004). These curves show the variation of matric potential [L] with change of the volumetric water content [$L^3\ L^{-3}$]. The matric potential represents the pressure of any water inside the soil's pores, attributed to capillary and adsorptive forces between the liquid and solid particles (Ritzema, 2006; Tuller & Or, 2004). It may be measured in any unit related to pressure, but is usually expressed in meters of a water column when depicted in a water retention curve.

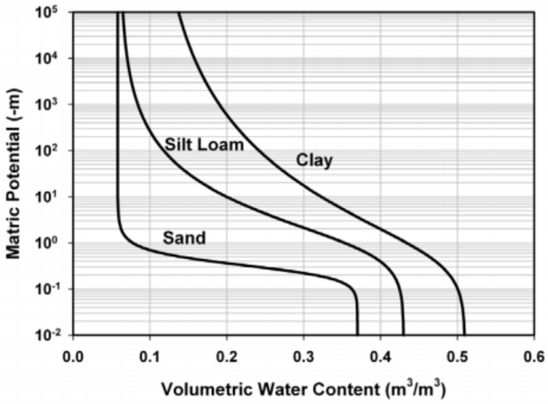

Figure 6: Example of soil water retention curves for sand, silt loam and clay. Note that the y-axis features a logarithmic scale. Reprinted from "Retention of Water in Soil and the Soil Water Characteristic Curve" by M. Tuller and D. Or (2004), *Encyclopedia of Soils in the Environment*, p. 1.

There are various models and empirical formulae available to plot a soil water retention curve, such as Brooks & Corey (1964), van Genuchten (1980) and Huyakorn et al. (1984). CATHY may be configured to use one of these different models. However, the specific version of CATHY that is used for LEO is set to use the van Genuchten model. This model is mathematically described by:

$$\theta(\psi) = \theta_r + \frac{(\theta_s - \theta_r)}{(1 + (|\alpha\psi|)^n)^{\frac{n-1}{n}}} \quad [3]$$

where ψ is the matric potential [L] and α is an empirical parameter scaling to the matric potential [L^{-1}]. More specifically, the inverse value α^{-1} [L] indicates the matric potential at the inflection point of the soil water retention curve and thus represents the capillary fringe (Van Genuchten & Nielsen, 1985). Because of this physical meaning of α^{-1} and the fact CATHY uses α^{-1} as input rather than α, values of α^{-1} are reported throughout this thesis. It is imperative to note that the variables θ_r and θ_s can be found quite easily through laboratory experiments. The parameters α^{-1} and n, on the other hand, have to be determined empirically by means of analyzing observed data.

2.2 Data acquisition

The collection of data is paramount in a large-scale controlled environment such as the one LEO is located in, which is why a wide array of sensors and samplers is present. Data collection and analysis is a cornerstone of this research, so the following section is attributed to the manner in which data acquisition is accomplished at LEO. Section 2.2.1 describes the sensors most important to this research – which are only few compared to all sensors available. Section 2.2.2 then provides an overview of the data sets which were used in this research and presents the reasons for choosing which set for which research purpose.

2.2.1 Sensors and samplers

Each hillslope within LEO comprises more than 1,700 different sensors and samplers to monitor quantities such as soil temperature, discharge rate, mass, wind speed, etc. As stated in section 2.1.2, these sensors are located at different depths measured from the soil surface. In fact, sensors are installed at all layer levels presented in section 2.1.1: –0.05 m, –0.2 m, –0.35 m, –0.5 m and –0.85 m. The number of sensors differs per depth, as does the exact lay-out of these sensors. An overview of sensor lay-out at different depths can be found in Figure A1 in Appendix A: experimental set-up.

Five kinds of sensors measuring four different variables are interesting for this research. Their properties are described below.

The volumetric water content in each hillslope is measured every 15 minutes using 596 5TM sensors. These sensors are to be found ubiquitously throughout each hillslope layer and present the soil moisture in percentages. The number of 5TM sensors decreases gradually from the top layer (154 sensors) to the bottom layer (34 sensors). This allows for maintaining a 1 to 2 meter resolution along the x- and y-axes of the slopes and even smaller resolutions along the z-axis (Pangle et al., 2015).

Hillslope discharges are measured with two different kinds of sensors, being calibrated NovaLynx tipping bucket gauges and magnetic flow meters (PE102 Flow Meter). They both register the discharge in liters over 15 minute time steps and they are installed at the same locations at the down end of the slopes (symmetrically, at (–4,0), (–2,0), (–1,0) and their positive counterparts), beyond the seepage face. The difference between both sensors lies in their reliability for respectively low and high discharge flows. The NovaLynx sensors are set up for measuring low flows and will typically underestimate higher discharge values. In turn, the PE102 sensors tend to be less reliable in measuring low discharge flows, as they are calibrated for higher values (from about 0.15 L min^{-1}).

The total system mass of each hillslope is measured using ten load cells. When their results are added up, these sensors give information about the total system's mass in kilograms. Like all the other sensors, the load sensors were set up to record the mass every 15 minutes. In- and outflows of the system in terms of mass can therefore be easily derived from the mass change over time.

Finally, the matric potential is determined by MPS-2 sensors. These are installed at the same locations as the previously named 5TM sensors and record the matric pressure every 15 minutes in kPa.

2.2.2 Data sets

The data analyses performed as part of this research are based on five rainfall-runoff events which were conducted during the May/June period in 2015. These experiments were chosen because they were conducted in a similar way for both the central and west hillslopes. An overview of elementary properties of these experiment series can be found in Table 1.

Table 1: Overview of elementary properties of data series used. The letters A through E are used throughout this document to designate the different experiment series.

Series	Time frame central slope (MST)	Time frame west slope (MST)	Rainfall duration (hours) (central/west)	Total rainfall (mm) (central/west)
A	11/5/15 07:30 20/5/15 23:30	18/5/15 07:00 27/5/15 23:00	12:00 / 11:55	134 / 134
B	26/5/15 07:30 29/5/15 07:00	2/6/15 08:15 5/6/15 07:45	12:00 / 12:00	134 / 134
C	29/5/15 08:30 1/6/15 03:30	6/6/15 11:30 9/6/15 06:30	6:20 / 6:06	63 / 63
D	1/6/16 09:00 4/6/15 06:00	10/6/15 12:30 13/6/15 09:30	7:13 / 6:45	74 / 74
E	4/6/15 09:00 10/6/15 21:00	14/6/15 12:00 21/6/15 00:00	6:52 / 6:53	72 / 72

As can be seen in Table 1, series A is almost identical for the central and west slopes in that its duration and total precipitation are very similar. Moreover, it is the only event with a long duration (12 hours of precipitation at a constant intensity), which has a large time frame, because no other experiments were scheduled immediately after series A. This allows for monitoring the slopes' behavior during the recession phase well. In addition, the hillslope initial conditions are similarly dry in this series. However, discharge data from the central slope in series A may be flawed due to serious clogging of the seepage face. This error is subject to a more elaborate description in section 5.1.2. Nonetheless, series A was chosen to be the most representative and unambiguous data set to assess the actual differences in response between the central and west slopes, mainly because of the similarity in initial conditions. The importance of comparable initial conditions for event-based simulations such as LEO has often been emphasized (e.g. Loague & Vanderkwaak (2002); Stephenson and Freeze (1974)).

3 Computational model

This chapter describes the basic principles of the computational model CATHY which was used during this research to simulate the two hillslopes. The first section entails a general description of CATHY and its position in the field of hydrology as compared with other hydrological models. Section 3.2 then serves as a rough outline of the simulation process which forms the core of CATHY. Finally, sections 3.3 and 3.4 respectively treat the required model input and its output. It is important to note that the sections 3.2 through 3.4 provide the reader with only a very rough description of CATHY sufficient to understand its role in this research project. Readers who seek a more complete description of CATHY may want to resort to other literature (e.g. Paniconi & Putti (1994); Paniconi & Wood, (1993)).

3.1 General description

Hydrological computer models found their very first introduction in the late 1960s. Since then, many new models have been built and proposed for a wide range of purposes and applications. Several studies have attempted to classify these models into certain classification schemes (e.g. Clarke, 1973; Todini, 1988). According to the most recent and elaborate categorization (Kampf & Burges, 2007), CATHY can best be classified as a distributed physically based model, because it numerically solves nonlinear partial differential equations for mass conservation and flow momentum (Camporese et al., 2010). As opposed to conceptual models, it does not oversimplify governing equations and boundary conditions at the cost of higher computational demands. Moreover, CATHY was designed to be applied to relatively small-scale study areas such as a hillslope or modest catchments and describe water flows in them. The version of CATHY in use at LEO simulates subsurface flow only, because overland flow was not supposed to occur during experiments conducted so far. Though some overland flow was reported during east slope experiments, no surface flow was observed in the central and west slope experiments.

The ultimate goal for the computer model in use at LEO grounds is to provide a greater insight in the relations and properties of natural coupled processes within watersheds. Numerous studies have made an endeavor to elucidate these coupled processes using models similar to CATHY (e.g. Graham & Butts, 2005; Singh & Bhallamudi, 1998). However, as opposed to these two examples, CATHY does solve the Richards equation in three dimensions, adding to the model's accuracy and complexity (Camporese et al., 2010). Additionally, CATHY can easily be coupled with other hydrological models, such as NOAH-MP which is capable of modeling overland flows, creating a powerful tool which enables LEO researchers to describe all water flows within the system. As stated before, however, this research only deals with subsurface water flows, so the sole use of CATHY suffices.

It can be concluded that CATHY is a suitable model to use at LEO. CATHY seems to fit its scale and goals well, and it may be coupled with other hydrological models to describe surface flows and transport of soil particles and solutes (e.g. Scudeler et al., 2016). This is especially convenient in a project involving a multitude of research disciplines.

3.2 Simulation

The subsurface module of the model is based on a solution of the 3D Richards equation (Richards, 1931). In the case of LEO, CATHY works with an evolved version of the Richards equation which also accounts for variably saturated porous media (Camporese et al., 2010; Niu et al., 2014):

$$S_w S_s \frac{\partial \psi}{\partial t} + \varphi \frac{\partial S_w}{\partial t} = \vec{\nabla}\left[K_s K_r(\psi)\left(\vec{\nabla}\psi + \vec{\eta}_z\right)\right] + q_{ss} \quad [4]$$

where $S_w = \theta/\varphi$ represents the relative soil saturation [$L^3\,L^{-3}$], φ is the porosity [–], S_s is the aquifer specific storage coefficient [L^{-1}], t is the time [T], ∇ is the gradient operator [L^{-1}], K_s is the saturated hydraulic conductivity tensor [$L\,T^{-1}$], $K_r(\psi)$ is the relative hydraulic conductivity function [–], η_z is a unit vector (0, 0, 1) with z measured vertically upward [L], and q_{ss} is the surface-to-subsurface contribution [L^3/L^3T]. CATHY solves the equation numerically using Galerkin finite elements. Details of this process, however, are beyond the scope of this thesis. Equation [4] does echo some of the most important input parameters that CATHY uses, which are treated in the section 3.3.

Time stepping in CATHY is adaptive in that it depends on the number of iterations required to reach acceptable convergence of Galerkin approximations. This means that simulated time steps which require only two or three iterations have a maximum time step of 180 s. This is the case throughout most of the experiment. During rainfall, however, CATHY may need more iterations to reach an acceptable solution and will automatically scale down time stepping in an effort to preserve simulation accuracy. A downside of this technique is that simulated values often cannot be directly matched to observed values in time, because time stamps differ. For instance, observed values are recorded every 15 minutes, while CATHY does not necessarily generate output every 15 minutes.

The spatial discretization of the hillslopes' soil was adopted from the east slope experiments by Niu et al. (2014). As can be reviewed in Figure 7, the 30 × 11.15 × 1 m slopes were discretized into a grid of 60 × 24 cells and 8 layers. To be able to resolve infiltration and seepage better, higher resolutions (0.05 m) were assigned to the surface and bottom layers of the slopes. Unlike time stepping, this spatial grid in the slopes does not vary based on the number of iterations necessary to reach convergence and is thus constant throughout the experiment.

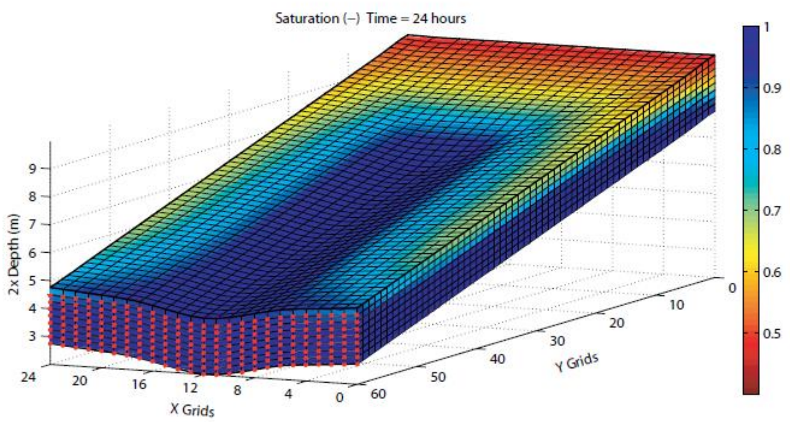

Figure 7: Discretization of hillslope soil with a grid of 60 x 24 x 8 cells. Note that the vertical depth is exaggerated by a factor 2 for clarity. The red dots at the slope's toe indicate the slope's seepage face. Color indicates the modeled degree of saturation in an east slope experiment and is not relevant here. Reprinted from "Incipient subsurface heterogeneity and its effect on overland flow generation – insight from a modeling study of the first experiment at the Biosphere 2 Landscape Evolution Observatory" by Niu et al. (2014), *Hydrology and Earth System Sciences*, p. 1877

3.3 Model input

CATHY first requires a detailed representation of the study area's geometry. The slopes in LEO are geometrically identical and have been captured in a Digital Elevation Model (DEM). CATHY uses this DEM to determine where water tends to go by calculating potential energies of the water at different levels. Naturally, the slopes' two-dimensional area and soil thickness are important as well.

Soil characteristics are also of great importance to CATHY's functioning. The user may decide which nonlinear characteristic relationship is used, such as the Van Genuchten model. This choice consequently influences some of the soil parameters necessary. For instance, α^{-1} and n are typical to the Van Genuchten model and are tied to the choice of this model. Also, the soil's hydraulic conductivity and its initial conditions in terms of matric potential (and thus soil moisture) are input of the model.

Naturally, CATHY will not work properly in LEO without any information on the rainfall event which takes place. Rather than the plain rainfall rate, CATHY uses the effective precipitation (*P*–*E*) for its simulations. Though not directly measured, the evaporation rate *E* may be found from the water balance as treated in section 2.1.5. Because the experiments at LEO were designed not to generate any surface runoff, no overland flow was observed and CATHY assumes that all rainfall infiltrates. To draw a valid comparison between the modeled and observed rates, observed values of storage, effective precipitation and discharge are entered as well. An overview of all the input parameters relevant to this research can be found in Table 2.

Table 2: Overview of input parameters and their units relevant to this research

Input parameter	Unit
α^{-1}	m
n	–
$K_{s,1}$	m s^{-1}
$K_{s,2}$	m s^{-1}
θ_s	–
θ_r (assumed 0)	–
Initial conditions (ψ)	–m
P_{eff}	m s^{-1}
S_o	mm
Q_o	m s^{-1}

3.4 Model output

After the simulation is completed, CATHY saves the modeled storage and discharge into separate files. These contain the variable time steps CATHY has used and the storage and discharge among other quantities. The results may be plotted to assess model performance qualitatively. To analyze the results quantitatively, the output needs to be post-processed in order to deal with the dissimilar time steps. This method is described in more detail in the next chapter.

4 Methodology

In this chapter the research methodology that was applied is illustrated. This chapter's structure is in accordance with the research questions that have been formulated. This means that each of the subsequent sections treats the methods utilized to answer one of the research questions. Section 4.1 describes how data was retrieved and analyzed to answer the first research question. The manner in which was determined what parameters would be most relevant to this research is explained in section 4.2. Section 4.3 then throws some light on the way CATHY was used to test whether the east slope's response is similar to the central or west slopes' responses. Just after, in section 4.4, the methodology employed to calibrate the model for both slopes is elucidated. Finally, section 4.5 describes how the found mathematical outcome relates to actual physical differences among the slopes.

4.1 Data analysis

In order to assess the size of the problem subject to research and to answer the first research question, data was obtained from the LEO database. This section is divided into three subsections. First the methodology to obtain an S,t plot, which visualizes the slopes' total water storage over time, is described. Just after is explained in which manner the Q,t plot was obtained, with *Q* representing the slope outflow, or discharge. In the third subsection the methodology used to obtain the soil water retention curves is highlighted.

The number of previously conducted experiments which are similar in duration and season for the central and west slopes is limited to five, of which two are suitable for a longer term analysis (> 72 hours). Therefore no attempt was made to compare the west and central slopes' performances statistically but rather hydrologically. One may expect resulting observations to be approximately equal given the slopes' presumed identicalness. The existing differences were analyzed and thoroughly described, and conclusions as to the size of the problem were drawn on the basis of the available data. Note that data from experiment series A was used for all analyses. S,t and Q,t plots for other experiment series are available in Appendix B.

4.1.1 Analysis of water storage over time in central and west slopes

Because there are no sensors in the hillslopes which directly measure its water storage, two different approaches were considered to find the slopes' water storage at different points in time. This could be done by using data from the load cells, which measure each hillslopes' mass and record this every 15 minutes. Changes in water storage could then be deducted from mass increments and decrements. Another method would concern using the volumetric water content data reported by the 5TM sensors. These sensors measure the soil moisture every 15 minutes and present it in percentages. Averaging these percentages for each layer while taking the number of sensors per layer into account would be a viable way to obtain the water storage in m^3.

It was eventually decided to use 5TM sensor data and choose the latter method to compute the water storage. The load cell data was known to fluctuate transiently on several occasions during previous experiments. For instance, data appeared to be rather noisy for several hours every time the artificial rainfall was either started or stopped. As of yet, the cause of this anomaly is unknown, so the problem continues to exist. Furthermore, load cells cannot account for any evaporation of water that is not yet fully infiltrated. In other words, they register temporary ponding at the slopes' surfaces as water storage, whereas water in these ponds may partly evaporate before it actually infiltrates into the soil and counts as water . 5TM sensors, on the other hand, are incapable of measuring the volumetric water content

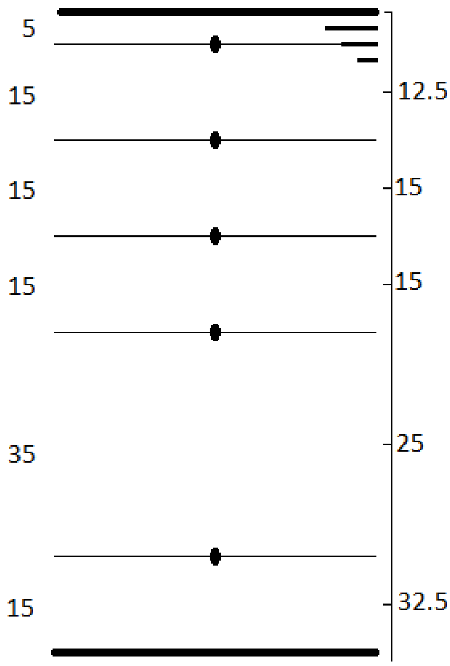

Figure 8: Overview of soil layers and their weighting partitions, as well as their corresponding depth levels below the surface. Depths in cm.

directly after precipitation lands on the hillslope. This is due to the fact that they are buried at several soil depths (at least –0.05 m). In spite of this disadvantage it was still deemed more beneficial to use 5TM data in order to avoid having to deal with noisy data in each experiment.

Some 5TM sensors did not function properly during the experiments in that they would either give sudden null values or negative values. These entries were manually removed from the data. Moreover, some sensors read values exceeding the soil porosity. The soil used in the east slope was tested for its porosity in a laboratory in 2014 and found to be 0.39 (Gevaert et al., 2014). The porosity for the central and west slopes had never been determined before, however. This was done by means of calibration of the porosity in the volumetric water content method to match data collected from the load cells. This method compared the sum of squared errors of water storage as found using the volumetric water content to the load cell data, solving for the porosity. A similar approach was employed by Gevaert et al. (2014) for the east slope. Despite the considerable number of malfunctioning sensors, the great multitude of sensors available guarantees reliable data, since the number of remaining sensors (around 500, depending on slope and experiment series) comfortably exceeded the minimum number required to draw solid statistical conclusions. A previous study approximated that valid statistical conclusions might still be drawn when only about 100 5TM sensors were still functioning accurately (Pasetto et al., 2015).

Because the number of 5TM sensors varies per slope soil layer, as was described in section 2.2.1, first the average volumetric water content per layer was calculated. Then the average of the complete slope was found by multiplying these averages by weighting factors compliant with the soil layer's thickness. These layer partitions, which may be reviewed in Figure 8 for clarity, have a depth corresponding half the depth of both the overlying and underlying levels. This manner allowed for reliable approximations of the total volumetric water content inside the hillslopes in m^3. These values were finally converted to values in mm.

4.1.2 Analysis of discharge rates over time in central and west slopes

As described in section 2.2.1, two different kinds of flow meters are in use at LEO, being the NovaLynx tippet buckets (low flow rates) and PE102 (high flow rates). To optimize data accuracy, data from the former devices was used to measure discharge rates while the precipitation event was still running (between 0 and 12 hours into the experiment). When precipitation was no longer being cast, the PE102 sensors were used to measure the discharge, because outflow rates then started to exceed the maximum value for which the NovaLynx tipping bucket gauges are considered reliable. The total discharge per time step of 15 minutes was acquired by adding up the readings of all six discharge sections and was plotted against time in Q,t plots. Also, the area under the Q,t curves was calculated to determine the total amount of water the slopes had discharged.

The Q,t plots were eventually used to draw conclusions as to the significance of the different responses observed in the central and west hillslopes. Because the number of experiments was too low (n = 5, of which only 2 involved measurements over a longer period of time), it was not possible to draw statistically sound conclusions. However, the similarities and differences observed from the results were used to compare the slopes in a hydrological sense, assuming the two slopes are fully identical.

4.1.3 Analysis of soil water retention curves of central and west slopes

Besides the water storage and outflow rates of both slopes, there is another important hydrologic characteristic that may be analyzed, being the soil water retention curve. The properties and meaning of this were discussed in section 2.1.7. Volumetric water content data was readily available from the water storage calculations and matric potential data was available by virtue of the widespread installation of MPS-2 sensors throughout each slope.

In order to obtain a good representation of the soil characteristics of both hillslopes, four different soil water retention curves were plotted. The first one depicts the average θ-ψ relationship in both slopes in time. In other words, for each time step of 15 minutes, the average value of both the volumetric water content and the matric potential throughout each slope was calculated. If reliable data was not available for either the volumetric water content or the matric potential, all data from that sensor location was disregarded. Both slopes' pairs were then plotted in the same figure. All observations with a volumetric water content above 0.20 m^3/m^3 were disregarded because of the MPS-2 sensors' inability to reliably measure matric potential in saturated conditions. Subsequently an attempt was made to fit the Van Genuchten model to both observed series by minimizing the sum of squared errors between modeled and observed volumetric water content values. In this process, the porosity was kept constant at 0.395, the value found using the method described in section 4.1.1. The residual soil moisture content θ_r was assumed negligible. This procedure revealed the values for the Van Genuchten parameters α^{-1} and n which best fit the observed data.

Additionally, another soil water retention curve was plotted using separate and non-averaged data from all available sensors in the Cartesian coordinate system of each slope, insofar the sensors worked properly. The remaining pairs of volumetric water content and matric potential were then partitioned (''binned'') in intervals of $\Delta\theta \approx 0.05$, depending on the number of pairs falling into that particular interval. It was decided to use volumetric water content data to categorize the pairs rather than the matric potential, because the former data series was thought to be the less accurate of the two. The number of pairs falling in each interval was tried to be held approximately constant in an endeavor to safeguard accuracy. This led to a total of 31 intervals for each slope. For each of these intervals, the average matric potential was calculated and these averages were subsequently plotted against the median value of each θ-interval. Error bars indicating the standard deviation of both the volumetric water content and matric potential for each interval were included as well. Finally, the Van Genuchten soil water retention curve was fitted to both sets of observed values to find the best fitting values of α^{-1} and n. This procedure was identical to the one described in the previous paragraph.

A similar technique of binning soil moisture data was used to obtain separate water retention curves of the soil in the five different slope layers and in five different zones. While the layer-wise analysis of soil characteristics aimed to uncover any variation in the slopes' z-direction, the five zones were defined in the x,y-plane, disregarding soil depth. The exact location of these zones can be found in Figure 9. The zones were defined according to their convergent nature. Zones 1, 2 and 3 converge all to the same point (0, 18) in the grid. Zones 4 and 5 converge to the line x = 0 and of course to the origin of the grid. Any sensors on the line y = 18 were allocated to zone 4 or 5. Any sensors on the line x = 0 and y < 18 were disregarded. The same method as described in the previous paragraph was

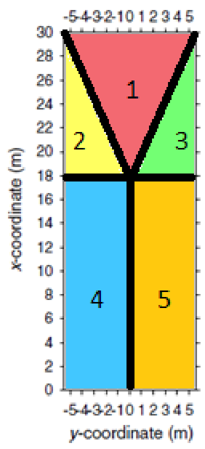

Figure 9: Overview of distinctive zones 1 through 5 in both hillslopes.

employed to find separate soil water retention curves for each layer and zone in pursuit of any notable differences in soil water retention characteristics among soil layers and zones. The Van Genuchten model was again fitted to the observations, finding optimal values of the parameters α^{-1} and n.

4.2 Most relevant parameters

As was described in the introduction of this thesis, it is impossible to carry out a full sensitivity analysis for CATHY to determine which parameters could be responsible for the difference in water retention times. Not only would this be too time consuming and unnecessary in light of this project's research aim, it is also considered to be very burdensome and challenging because of CATHY's complex and highly nonlinear nature. Instead, the number of parameters subject to research must be narrowed down to be able to investigate the source of the observed differences within time constraints while preserving maximum accuracy. In other words, a delicate balance between the number of parameters involved in further research and its outcomes in terms of reliability had to be struck.

To decide which parameters would be most interesting to focus on, a literature study was conducted as well as an interview with Dr. Troch. Previous studies on LEO (e.g. Gevaert et al., 2014; Niu et al., 2014; Pangle et al., 2015; Scudeler et al., 2016)) had already described and analyzed various characteristics of the LEO hillslopes and equipment on-site. Judging by their conclusions and assessments of LEO, four different cornerstones of the project's reliability were defined: equality of the slopes' geometry, experiment set-up, measuring equipment and soil characteristics. These cornerstones were then broken down into specific separate criteria which, when somehow compromised or dissimilar in the central and west slopes, might be responsible for the differences in observed responses.

All these key aspects were then elaborately examined to conclude whether or not they would be likely to be capable of bringing about a discrepancy in observations of the magnitude that was observed. When two criteria had been proven to be similar or alike, further investigating them was considered not to be very fruitful as those criteria would be unlikely to be responsible for the research gap. On the other hand, criteria which had shown considerable variation during past studies or had been found not to be alike, became more interesting to shift focus to.

Eventually three soil characteristics were found to examine more closely for the remainder of the research, being the Van Genuchten parameters α^{-1} and n and the hydraulic conductivity K_s. A more elaborated description of the rationale involved can be found in section 5.2. The parameters are only briefly mentioned in this section because of their importance in the upcoming sections.

4.3 Computer model analogy for central and east slopes

Before the actual determination of the values of α^{-1}, n and K_s in the central and west slope, it would be interesting to see what results can be generated if east slope input parameters are used to simulate the central and west slopes in CATHY. Niu et al. found specific values of these parameters in 2014 during their study in which CATHY was calibrated for an east slope experiment. Though they concluded that the east slope's initially homogeneous soil had probably transformed into heterogeneous soil due to the occurrence of overland flow, these input parameters may generate accurate simulations of the central and west slope responses. After all, scientists at LEO have formulated the hypothesis that the central slope's response is very close to the east slope's response from preliminary hydrological analyses. If east slope input parameters are indeed capable of predicting either the central or west slope response well, it is not necessary to calibrate CATHY separately for that particular hillslope. In that case east slope parameters may be assumed to simulate that specific slope and be used to explain how the third slope differs from the former two which respond more or less equally.

To test whether or not using east slope input parameters yields accurate simulations of the central and west slope, two base runs were simulated in CATHY. To do so, CATHY was configured according to optimal east slope input parameters as found by Niu et al. (2014). An overview of these parameters may be found in Table 3. In line with optimal east slope model performance, both hillslopes were divided into two zones featuring their own value of the hydraulic conductivity K_s to reflect the soil heterogeneity Niu et al. (2014) found. The hydraulic conductivity of the soil nearby the seepage face was assumed to have a value of $2.2{\cdot}10^{-5}$ m s^{-1}, approximately 10 times smaller than the $K_{s,1}$ of $1.4{\cdot}10^{-4}$ m s^{-1} assumed across the rest of the hillslope. Initial conditions in matric potential are experiment-bound and therefore did have different values across the three experiments. The values for these initial conditions were found by averaging the readings from MPS-2 sensors for each of the five layers separately. These averages were then weighted by the thickness of their adjacent layers, similarly to the method used to find the storage from volumetric water contents. This method is only reliable when the slope is in a dry state prior to the experiment as was the case, since saturation of the MPS-2 sensors measuring the matric potential drastically lowers their reliability.

Table 3: CATHY configurations as found for the east slope according to Niu et al. (2014) and used to generate a base run for the central and west slopes.

	Niu et al. (2014)	Base run
α^{-1} (m)	–0.6	–0.6
n (–)	2.26	2.26
$K_{s,1}$ (m s^{-1})	$1.4 \cdot 10^{-4}$	$1.4 \cdot 10^{-4}$
$K_{s,2}$ (m s^{-1})	$2.2 \cdot 10^{-5}$	$2.2 \cdot 10^{-5}$
ic (m) (central/west)	Unknown	–0.8255/ –1.2164
θ_s (m^3 m^{-3})	0.3675	0.3675
θ_r (m^3 m^{-3})	0.002	0.002

To obtain accurate model results, it was necessary to correct the sudden inconsistency in the discharge data for the central slope observed at 25 hours into the experiment. Due to partial clogging of the seepage face, one out of six discharge meters consistently reported lower discharge values for a period of about 13 hours. This issue is discussed in more detail in section 5.1.2. Because of this clear anomaly in observations, it may be expected that model predictions would be very different at this time. This was confirmed by comparing observed and simulated results before any correction of data had taken place. To draw a fair comparison between the simulations and observations, the observed discharge data was corrected upward between 13 and 25.5 hours. To accomplish this, storage data from load cell measurements was used. Unlike the storage data acquired from soil moisture measurements, load cell data was influenced by the seepage face clogs because it measures the total system mass rather than soil moisture at fixed points. This storage data in conjunction with the assumption that the evaporation is negligible was then used to compute the actual discharge rate Q for every time step from the water balance. Since the discharge data which needed correction was gathered mainly during the night (between approximately 20:30 and 09:00), it was considered acceptable to neglect evaporation rates. The subtraction $\Delta S_L – \Delta S_M$ (with L indicating load cell data and M indicating soil moisture data) consequently allowed for calculating the amount of water that had been stuck behind the clogged seepage face every time step. This value was added to the discharge meter at the clogged section. Any retardation which is normally present between the storage and discharge is thought to be minimal, since the water built up right at the seepage face where discharge takes place. The result appeared to be in line with expectations.

This method was considered the best option in light of the circumstances. Because initial storage conditions between the two slopes are very different in the series B experiment, this event would not have been ideal to use in simulations either. In this data series, the west slope’s water storage is about 20% higher than in data series A, making it more difficult to approximate initial conditions due to the sensors’ inability to read reliable matric potential values in saturated conditions. Besides, discharge data from series B also showed some seepage face clogging, albeit less so.

Before simulating the specified case with CATHY it was decided to use two different model efficiency coefficients to assess the model performance in terms of a goodness-of-fit coefficient which fits the modeling objective. In line with common practice in hydrology, the Nash-Sutcliffe coefficient was used to quantify CATHY's simulation capabilities. This model efficiency coefficient was chosen because of its widespread use in hydrological research and its flexibility in that it may be used for a wide range of input variables, among which the discharge and storage. Furthermore, the American Society of Civil Engineers recommends using the Nash-Sutcliffe coefficient for hydrological purposes (ASCE, 1993) and it was found to be the best method of model assessment in case of rainfall-runoff modeling (Dezetter & Servat, 1991). The Nash-Sutcliffe coefficient is usually written as follows (Nash & Sutcliffe, 1970):

$$NSE = 1 - \frac{\sum_{t=1}^{T}(Y_o^t - Y_m^t)^2}{\sum_{t=1}^{T}(Y_o^t - \overline{Y_o})^2} \quad [5]$$

where *NSE* is the Nash-Sutcliffe model efficiency coefficient [–], Y_o^t is the observed value of quantity *Y* at time *t* [T] and Y_m^t is the modeled value of quantity *Y* at time *t*.

However, using the *NSE* does have some disadvantages, the most important of which is its tendency to be overly sensitive to relatively low and – even more so – high observed values. The cause of this lies in the fact that differences between observed and modeled values are squared, emphasizing errors at high and low values. It is therefore recommended to combine different model assessment quantifications (Krause et al., 2005). As such, the Kling-Gupta coefficient was also calculated to compare modeled with observed values (Gupta et al., 2009):

$$KGE = 1 - \sqrt{(R-1)^2 + (\frac{\sigma_m}{\sigma_o} - 1)^2 + (\frac{\overline{Y_m}}{\overline{Y_o}})^2} \quad [6]$$

in which *KGE* is the Kling-Gupta model efficiency coefficient [–] and *R* is the correlation between the observed and simulated series of quantity *Y* [–].

Although Gupta et al. (2009) acknowledge that errors may still be overestimated when the *KGE* is computed for extreme values, they emphasize that the offset is significantly less severe. The *KGE* is therefore considered complementary to the *NSE*, which is the reason both model efficiencies were combined to measure CATHY's simulation performance. The total model efficiency accounts for both the discharge and the storage. This means in mathematical terms:

$$E = \frac{1}{4}\left(NSE_Q + NSE_S + KGE_Q + KGE_S\right) \quad [7]$$

Since both the *NSE* and *KGE* indicate a perfect match between simulated and observed values when their value is 1, the same applies to the newly defined coefficient *E*. The closer its value to unity, the better the model performance.

Because of the lack of preceding model experiments at LEO, it is difficult to determine a clear threshold distinguishing good model performance from bad performance. Though many studies consider a hydrological model to perform well when either the *NSE* or *KGE* (or both) is found to be at least 0.70 (e.g. Andersen et al., 2001; Ley et al., 2015; McCuen et al., 2006), this value is often subject to debate in other studies (e.g. Criss & Winston, 2008; Smith et al., 2008), especially in cases where quantities other than the discharge are considered. It was therefore decided not to set a clear-cut threshold of *E a priori* to evaluate CATHY's model performance but rather assess it afterward.

After the model had been run using the specified configuration, its output for both cases were visualized in S,t and Q,t plots, allowing for a qualitative analysis. The resulting model efficiency coefficients *E* were also included.

4.4 Computer model calibration

As will be shown in section 5.3, neither the central nor the west slope case was simulated accurately using east slope input. Because of this, CATHY was not readily available to mimic central or west slope observations precisely. In order to be able to reveal variations in α^{-1}, n and K_s between the central and west slope, CATHY had to be calibrated separately for both slopes given their respective sets of observations. This calibration process was done by optimizing the model efficiency coefficient E described by formula [7] based on the *NSE* and *KGE*.

As a first guess, the values for α^{-1} and n as found by analysis of the soil water retention curves were used in conjunction with a homogeneous value for K_s of $1.4 \cdot 10^{-4}$ m s^{-1} as used by Niu et al. (2014) to run a new simulation with CATHY to see if they would bear a better simulation result. Because this appeared to be the case (E was found to be respectively 0.888 and 0.821 in the central and west cases), these input parameters were considered the starting point for the subsequent calibration procedure.

The optimization process of E was achieved in two steps. In a preliminary analysis CATHY was run with random values from an assumed uniform distribution for broad ranges of α^{-1}, n and K_s. For the central slope, these ranges were respectively [–0.65; –0.2 (m)], [1.7; 3.3 (–)] and [$0.5 \cdot 10^{-4}$; $3.0 \cdot 10^{-4}$ (m s^{-1})], inspired by the analyses of the soil water retention curve and the results of Niu et al. (2014). Initial parameter ranges for the west slope were [–0.7; –0.25 (m)], [1.45; 2.8 (–)] and [$0.5 \cdot 10^{-4}$; $3.0 \cdot 10^{-4}$ (m s^{-1})], reflecting a higher approximated value of α^{-1} and a lower value of n as found by fitting the Van Genuchten model to observations. Each set of random variables was written to their respective input files in CATHY and the model was subsequently run. Modeled results were then paired up with observed results by interpolation of CATHY's results. This was necessary because CATHY's time stepping is adaptive, as was treated in section 3.2. However, the offset between observed and modeled time steps never exceeded 20 seconds, so linear interpolation was considered justified. This method was also applied in east slope study by Niu et al. (2014). Subsequently, a Fortran-script was used to calculate the *NSE* and *KGE* for each run and to average these. The resulting value of E was finally written to a separate file which also included the random input parameters. These processes were looped in Shell script to obtain 350 simulations.

The results of these simulations were visualized in three dotty plots, one for each variable and indicating the value of E as the input parameter varied, and in three color plots depicting E as two input parameters were varied. These figures, which may be found in Appendix D, were used to narrow down the calibration range for each variable, disregarding any input values which yielded negative values of E. Adapted ranges of [–0.4; –0.05 (m)], [1.55; 2.8 (–)] and [$1.2 \cdot 10^{-4}$; $2.5 \cdot 10^{-4}$ (m s^{-1})] (central) and [–0.7; –0.12 (m)], [1.7; 2.8 (–)] and [$0.9 \cdot 10^{-4}$; $1.8 \cdot 10^{-4}$ (m s^{-1})] for respectively α^{-1}, n and K_s were then programmed and used to generate a second set of 1.000 final results. The results were again portrayed in dotty and color plots to check if the used ranges of input parameters had been sufficiently broad.

The parameter sets which generated the best match between modeled and observed values (i.e. which yielded the highest value of E) were used to plot the simulated and observed responses in S,t and Q,t plots. To account for uncertainty, the 20 best fitting parameter combinations were plotted as well, complementing the plots with a bandwidth of uncertainty. Moreover, these 20 combinations were expressed in ranges for each parameter and each hillslope to be able to compare the two slopes properly.

The central and west slope were calibrated using the same scripts, albeit with slight modifications in initial conditions and of course observed values. Any differences between the two slopes should be echoed by significant variations in calibrated input parameters. These differences were examined and used to draw conclusions.

4.5 Underlying causes of found difference

Having concluded that mainly great variation of α^{-1} among the two hillslopes seems to be responsible for the different observations of water transit times (see section 5.4), an attempt was made to link this conclusion to the physical model and find out how this difference had come to exist. To see how the newly found optimal parameters would influence the soil water characteristic of both slopes, a theoretical soil water retention curve was plotted assuming the Van Genuchten model. This plot includes the water retention curves of the single optimal values and accounts for uncertainty, taking again into account the best twenty simulations. Of course this plot does not account for any spatial variability in the three parameters across the slopes, as soil homogeneity was assumed in the calibration procedure.

Since no unambiguous or unique physical cause could be found for the observed difference, a seminar was organized in which the results were presented and discussed with other researchers at LEO. This seminar did not only serve to inform LEO staff about this research's findings but they were also explicitly asked to share their opinion and help put forward any reasonable and testable hypothesis that would explain this research's outcomes. The general conclusion was that no clear cause of the observed difference could be found without further research. Instead, some hypotheses were formulated which may explain the found difference and support the results from this research. These hypotheses may be tested in future research projects and are presented in section 5.5.

5 Results

This chapter reports the research results which were found according to the same structure as was employed in chapter 4. This means section 5.1 contains a data analysis of the slopes' total water storage over time, discharge over time and soil water retention curves. Interpretations of these analyses are used in section 5.2 to choose the three most relevant parameters for further research, along with experts' opinions and conclusions from existing literature. Subsequently, results of the first model run using east slope input data in an effort to mimic central and west slope responses are treated in section 5.3, both qualitatively and quantitatively. Section 5.4 focuses on model calibration of CATHY for the central and west slope cases, optimizing the value of the goodness-of-fit coefficient *E* by varying the three input parameters. Finally, an attempt is made to elucidate in what sense the two hillslopes differ in section 5.5, using results from section 5.4.

5.1 Data analysis

As was described in Chapter 4, first it was attempted to assess how substantial the difference in water retention times between both slopes is. This involves analysis of data which was acquired during previous experiment series, named A through E. As stated in the previous chapter, series A serves as the representative series throughout this section. Some results for the remaining experiment series can be found in Appendix B and are cited if necessary.

Sections 5.1.1 and 5.2.2 present the results of data analysis of respectively the total water storage within the slopes and their discharge. The results are shown graphically in S,t and a Q,t plots. Also, details and peculiarities of these curves are described. The soil water retention plots for both slopes are covered in section 5.2.3, as well as interpretation of these curves. The chapter ends with a conclusion of the analysis done, answering the first research question.

5.1.1 Analysis of water storage over time in central and west slopes

As was treated in section 3.1.1, some 5TM sensors recorded volumetric water contents way above the presumed porosity approximation, which is physically impossible. These values were calibrated to match water storage results generated by the load cell method. This led to the conclusion that the porosity of both hillslopes' soil is about 0.395, in line with the east slope's porosity value of 0.39 reported by Gevaert et al. (2014). This value was adopted for the remainder of this research.

The total water storage inside the central and west slopes has been visualized in an S,t plot, to be found in the upper graph Figure 10. The difference in storage over time is also plotted in the lower graph of Figure 10. Both slopes have about the same initial storage of approximately 107 mm. It must be noted that precipitation starts immediately at 0 hours. From the graph it becomes clear that both slopes' water storage increases steadily to about 240 mm when rainfall is stopped at 12 hours into the experiment. The storage of both slopes continue to increase, albeit less so. This phenomenon may be explained by the experimental set-up in which the 5TM sensors are buried in the soil. The first layer of sensors is localized at –0.05 m from the surface, so registration of any water above this layer is somewhat delayed. The central slope reaches its maximum storage slightly earlier than the west slope: after 17 hours versus 21.5 hours. Having reached their tops, both curves start declining due to the precipitation water discharging through the seepage face at the toe slopes' toe.

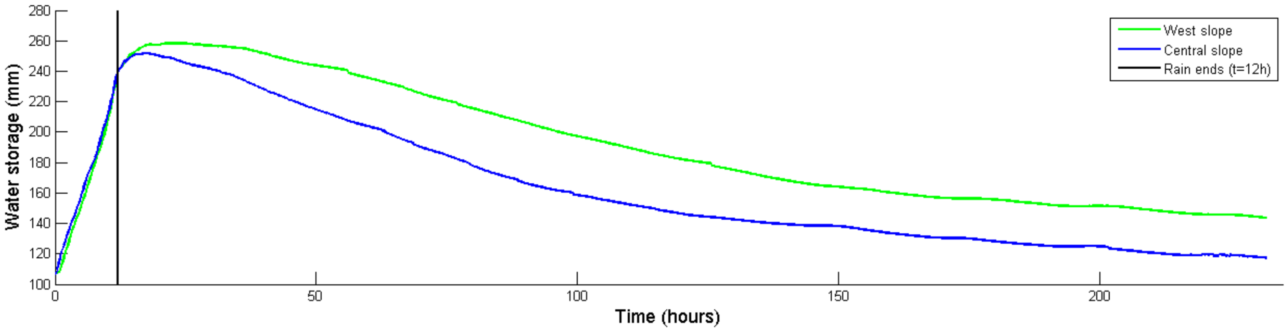

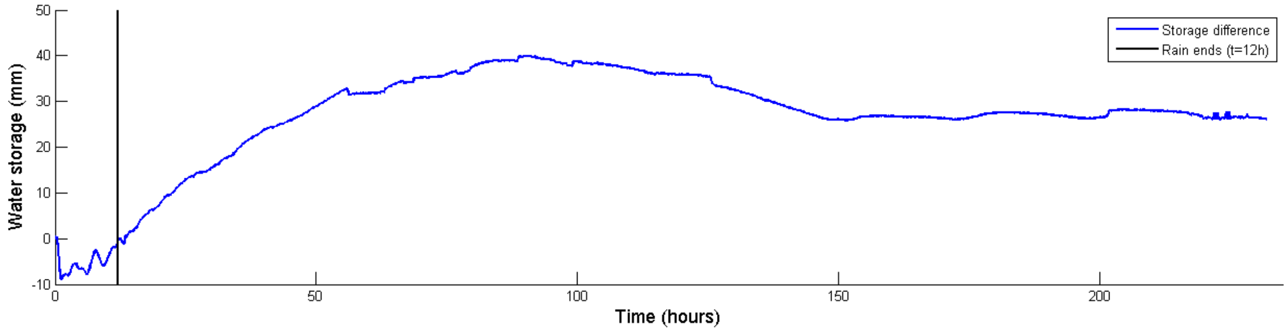

Figure 10: (upper): Water storage as function of time for the central and west hillslopes with data from experiments series A. (lower): The difference in water storage in both slopes over time.

It immediately becomes clear that the central slope loses its water faster than the west slope. The second graph, located in the bottom part of Figure 10, illustrates this as well. Here the central slope's storage is deducted from the west slope's storage, portraying their difference. This difference increases over time, reaching its top at around 90 hours into the experiment, but remains high during the entire following course of the experiment. Graphical analysis of storage over time for the other experiment series yield similar results (see Appendix B).

5.1.2 Analysis of discharge rates over time in central and west slopes

Figure 11 shows the discharge over time for both hillslopes in a Q,t plot. Again, precipitation starts immediately at 0 hours. Unlike the storage over time, the discharge remains low for a longer period. This is due to the fact that the outflow meters are located beyond the seepage face, down the hillslope. It simply takes some time for the water to discharge and reach these sensors. Flow rates do start to pick up as the rainfall ends, at 12 hours into the event. The first response is compatible with the observations described above from the S,t curve: the central slope loses its storage faster and its discharge rate is logically higher than the west slope's. Furthermore, the central slope's outflow rate soars up before the west slope's, after around 10 hours, indicating that water travel times are less within the central slope.

Special attention must be paid to the sudden bump in the central slope's curve at approximately 25 hours. Outflow rates decline moderately between 13 and 26 hours, only to increase sharply suddenly afterward. A glance at the data revealed that one out of six PE102 flow meters had registered lower outflow values, located at (0, –4) in the coordinate system. The same anomaly was visible for the NovaLynx tipping buckets. The shape of the curve at this point gave rise to the hypothesis that the seepage face somehow had partially gotten clogged at this point in the experiment. This would explain stagnating outflow rates and a surge upward as soon as the clog was removed. It would also reveal why no sudden changes in storage can be seen in Figure 10, as the water would build up right at the seepage face whereas the nearest 5TM sensor is located about 2 m slope upward, unable to measure any water stuck behind the seepage face. This hypothesis is supported by dr. Pangle, who recalled removing clogs at the very same location at the same time from his notebook. Some other experiment series also experienced similar clogging, not rendering them more useful for the purpose of data analysis (see Figure B3 in Appendix B).

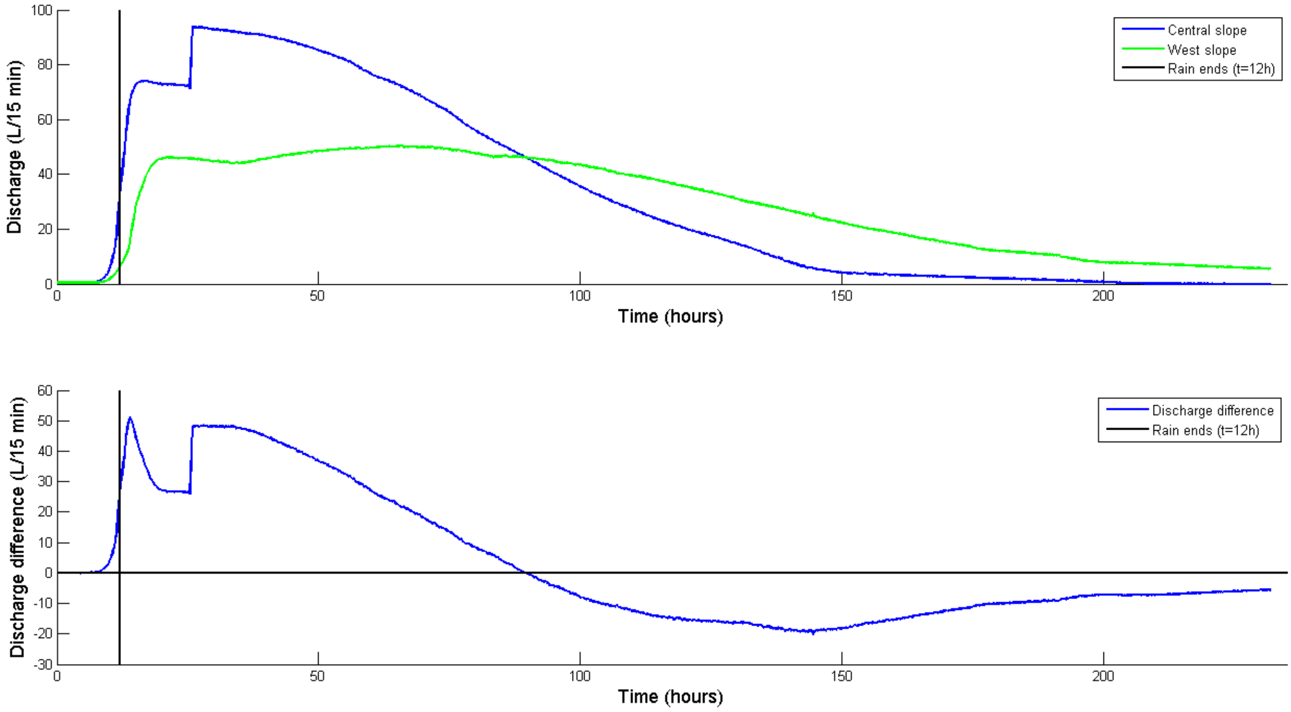

Figure 11: (upper): Discharge rates as function of time for the central and west hillslopes with data from experiment series A. (lower): The difference in discharge rates in both slopes over time (central slope discharge minus west slope discharge).

After around 90 hours, the curves intersect. From that point, the west slope's outflow rates are higher than the central slope's. At 200 hours into the event, the central slope's discharge rates halt, while the west slope continues to generate low outflow rates. It is important to mention that the total discharge of both flows over the course of this series is 29,100 L for the central slope and 26,450 L for the west slope. These values are likely to be similar eventually, since the west slope has not yet fully discharged at the end of the curve. Considering that 44,220 L of rainfall was cast on both slopes, the central slope's runoff coefficient is approximately 66%. This value seems to comply with the previously found ratio of 68%. Similar runoff coefficients were derived from other experiments, additional plots of which can be found in Appendix B.

5.1.3 Analysis of soil water retention curves of central and west slopes

The soil water retention curves depicting averaged θ-ψ pairs in both slopes for each time step (see section 4.1.3) can be found in Figure 12. Observations featuring a volumetric water content above 0.2 $m^3\,m^{-3}$ were disregarded because matric potential data is not reliable in saturated conditions. The modeled Van Genuchten curves have been fitted to observational data.

Several phenomena stand out in Figure 12. The recharge and recession phases can be clearly distinguished: during recharge the volumetric water content quickly increases, indicated by the scattered dots in Figure 12. The discharge process of both slopes is much slower, however, resulting in a greater number of observations. Also, it would seem that the water retention curve of the central slope lies lower than is the case for its western counterpart. In other words, at the same observed matric potential, the central slope's soil moisture is less than it is for its western counterpart. Reviewing the example soil water retention curve of section 2.1.7 (Figure 6), the conclusion may be drawn that the west slope's soil is less permeable than the central slope's. After all, the lower the curve, the more permeable its soil is.

Assuming values of 0.395 and 0 for θ_s and θ_r respectively, the optimal values for α^{-1} and n were calibrated using observational data. For the central slope, it was found that α_c^{-1} = 0.323 m and n_c = 2.22 generate the most accurate fit of the Van Genuchten model to the observations. Similarly, values of α_w^{-1} = 0.364 m and n_w = 1.94 were found for the west slope, reflecting well its different characteristics compared to the central slope.

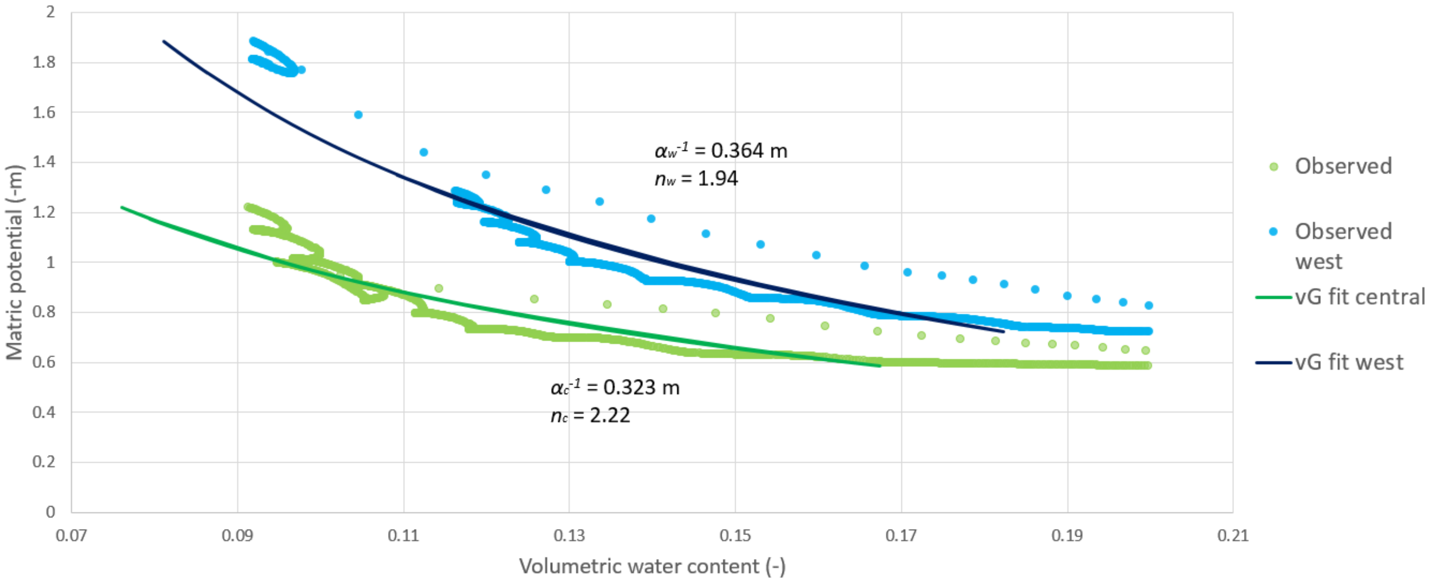

Figure 12: Soil water retention curves for the central (blue) and west (green) hillslopes. The scattered, light-colored dots represent observed values, whereas the solid lines visualize theoretical values calculated with the Van Genuchten model and fitted to observations. The fitted values for α^{-1} and n are included in the figure.

Interpretation of the other water retention curves, included in Appendix C, does not yield completely unambiguous results. Though they all indicate that the western slope's soil is less permeable than central slope soil because the latter's water retention curve lies significantly lower, the fitted values of the Van Genuchten parameters α^{-1} and n do show serious variation among the plots. For instance, the layer-wise analysis does support Figure 12's observation that α_w^{-1} is greater than α_c^{-1}, but at a different scale of 0.603 m versus 0.498 m. In contrast, point-wise and zone-wise analyses induce an opposite conclusion, since α_w^{-1} seems to be smaller than α_c^{-1} in these cases. Moreover, the west slope's soil shows greater variability among its different layers and zones, whereas observations seem to be more uniform throughout the central slope (see Figures C2 and C3 in Appendix C). Apparently the values of α^{-1} and n are difficult to be determined unambiguously and show considerable variation among methods, hillslopes and even across the individual hillslopes.

5.1.4 Conclusions

Although no valid statistical conclusions may be drawn because of a lack of samples and the difficulty involved in acquiring more, analysis of the three main hydrological properties has revealed a stark contrast between both slopes. It has become indisputable that the west slope retains water significantly longer than the central slope. The latter is capable of discharging at twice the rate of the former and starts losing water through discharge sooner. The difference in water storage surges from practically 0 mm at 0 hours to some 40 mm at approximately 90 hours into the experiment and stays significant for the remainder.

Additionally, the soil water retention curves are rather different for both slopes and their exact fitting parameters are even in disagreement across the individual slopes. All plots do have in common that they demonstrate a marked difference between the permeability of both slopes' soils. The west slope's soil appears to be less permeable, which may very well explain its tendency to retain water longer. Lower permeability causes lower discharge rates during the first part of the experiment in the west slope case. In turn, lower discharge rates mean that the total storage remains higher in the west slope. In spite of lower permeability, the west slope will most likely discharge approximately the same amount of water as the central slope, suggesting their runoff coefficients are about the same.

The S,t and Q,t trends do not deviate from results generated with the other data series B through E, as may be reviewed in Appendix B. All experiments yield the same result, rendering the west slope the slower in terms of discharge by a considerable margin. The uniformity in these event results and the figure by which both slopes' hydraulic properties differ leave no other possibility than to conclude that both hillslopes indeed differ significantly in hydrological terms when it comes to water retention times.

5.2 Most relevant parameters

In this section, the relevant computer model parameters to which this research's focus was shifted are presented, as well as the line of thought involved in reaching this conclusion. Figure 13 shows the breakdown structure that was used to categorize all the elements in each hillslope which in themselves may cause considerable differences in observed outcomes. When all the criteria are alike in both hillslopes (colored green in Figure 13), no different outcomes should occur.

With regard to the slopes' geometry it was thought that identicalness of three criteria would be important for the responses to be equal. The 2D area and the slope grade both depend on the steel structures below LEO's hillslopes (Pangle et al., 2015). These structures were designed and assembled using modern computers and machinery and are therefore ruled out of being the cause of the tremendous differences observed. The soil layer thickness, although proven to be slightly greater in the west slope, is not thought to be a probable cause of the observed difference either. The difference in soil thickness between the central and west slope is only about 2% and such difference would not be able to compromise the physical model's performance much (dr. P. Troch, personal communication, June 2016).

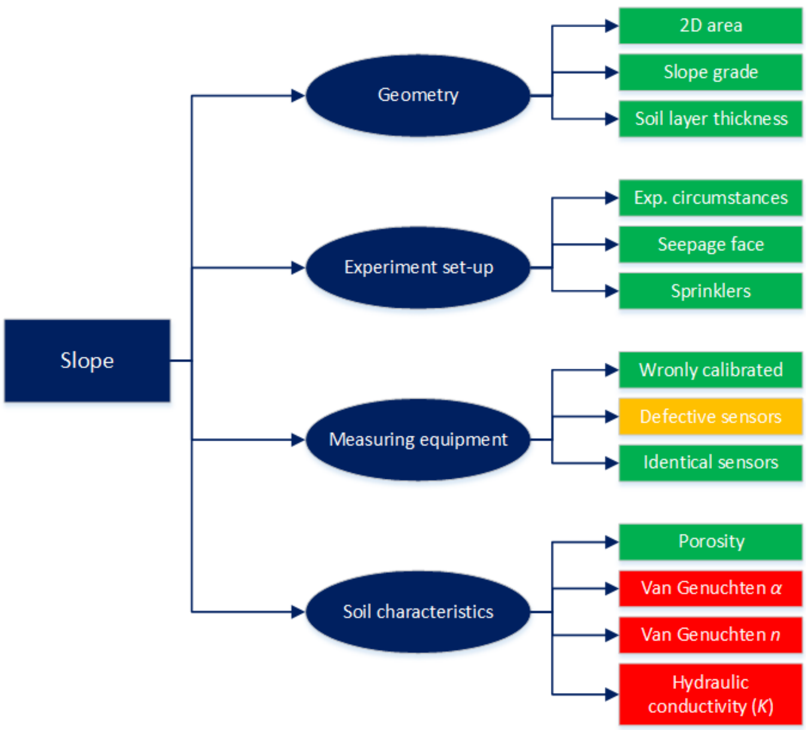

Figure 13: Overview of each hillslope's properties possibly responsible for the observed difference in water retention times. Green properties are considered to be proven alike for the central and west slopes, the yellow property indicates concern and similarity has not at all been established for the red properties.

Circumstances of the two experiment series that were examined were very alike. Both experiments were conducted in May 2015, lasted equally long and featured the same amount of precipitation cast on the hillslopes. Variations in the course of these experiments, if any, are thought to be minimal. Since the slopes' seepage faces and sprinkles were constructed equally and proved to function properly during tests, they need no further attention.

Though boasting an impressive array of state-of-the-art sensors in each hillslope, about 25% of the used sensors in the west slope showed defects of some kind. While worrying, especially so because of their virtual irreplaceability, Pasetto et al. (2015) found proof that the project will not be jeopardized by faulty sensor readings as long as at least 100 out of 596 sensors work properly in each slope. This is still the case by a generous margin, so the cause of the observed discrepancy should not lie in measuring equipment.

The soil porosity in both slopes was determined earlier in this research and was very alike in both cases at about 0.395. However, the soil water retention characteristics, α^{-1} and n have demonstrated major variations in the soil water retention curves. Not only did their values seem to differ between both hillslopes, wide variability was also observed throughout the individual hillslopes' zones and layers. Moreover, previous studies have indicated considerable uncertainty in both α^{-1} and n (such as Niu et al. (2014) and Hazenberg et al. (2016)). Because the hydraulic conductivity is partially governed by the pore-size distribution index n (see equation [2]), it would be interesting to study this parameter more closely as well.

Since so many aspects concerning the physical model's set-up and the experiment designs have been proven to be very much alike in both cases, it is logical to shift attention to the soil characteristics. These parameters have exhibited interesting variability during previous studies and continue to show considerable differences even across certain layers and zones inside the hillslopes. This gives sufficient reason to suspect that soil characteristics are indeed different in both hillslopes and may thus be responsible for the marked discrepancy in terms of water retention times that was observed.

5.3 Computer model analogy for central and east slopes

This section contains results obtained from the first CATHY model run in which was attempted to simulate central and west slope experiments using previously found east slope input parameters. The goal was to test whether CATHY would be able to simulate either the central or the west slope accurately using optimal east slope input parameters as found by Niu et al. (2014). If such were the case, it would be justifiable to assume east slope parameters as being representative for the central and west hillslopes for the remainder of the research. Scientists at LEO support the hypothesis that the central slope response resembles the east slope's response based on preliminary hydrological analysis.

The results of the CATHY simulation of the central slope using east slope input are visualized in Figure 14. The upper graph depicts the discharge as a function of time, the lower shows the storage as a function of time. Note that the observed discharge data has been corrected upward to account for the seepage face clogging. Also, the model efficiency coefficient E, as defined in equation [7], is included for both hillslope cases.

The Q,t and S,t plots indicate that there is a glaring discrepancy between central slope observed and simulated values. CATHY appears to reach higher discharge rates earlier in the experiment and discharges much more water than was observed. Also, the model overestimates the initial hillslope storage by a factor of about 2 (approximately 67 m^3 versus the measured 36.5 m^3) and is not able to compensate this overestimation despite higher discharge rates. This poor model performance is echoed by a disappointing model efficiency coefficient of 0.126.

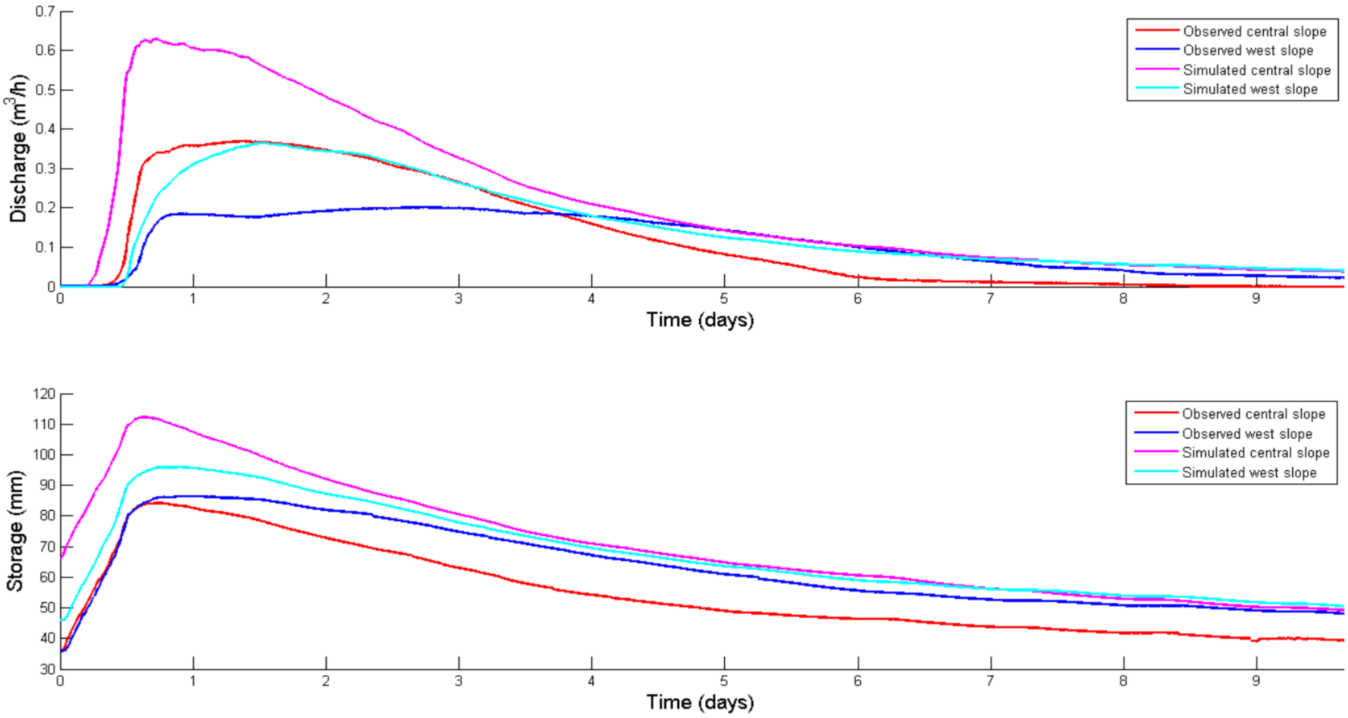

Figure 14: Output of CATHY simulations of the central and west slopes using east slope input parameters. The upper panel depicts discharge-over-time, the lower panel storage-over-time. The goodness-of-fit coefficient *E* is 0.126 in the central slope case and 0.679 in the west slope case.

The west slope simulation under east slope input seems to be closer to the observations. CATHY manages well to simulate the point in time at which discharge rates start to pick up and resembles observed discharge rates very well from four days into the experiment onward. However, it does greatly exaggerate discharge rates before then. As for the storage, the model estimates initial storage rates much better than in the central slope case, but still not very closely (about 46.5 m^3 versus 36.5 m^3 observed). For the remainder of the experiment, storage simulations are reasonably in line with observations. Although model performance is clearly better than in the attempt to simulate the central slope's response, the value of *E* in the west slope case is still only 0.679.

The results obtained from the computer model experiments vanquish the hypothesis about the central and east slopes' similarity which LEO researchers put forward. Judging by Figure 14 and the model efficiency coefficient of 0.126, CATHY's performance in simulating central slope observations under east slope input is very poor. On the other hand, the west slope does seem to bear more resemblance than was previously thought. In fact, one could conclude that the central slope is the outlier of the three hillslopes and not the west slope as was presumed.

Furthermore, these results indicate that neither the central, nor the west hillslope can be simulated reliably when east slope input is used in CATHY. Though its performance is much better in the west slope case than in the central slope case, this distinction is merely relative. CATHY's simulation of the west slope is still not very accurate when compared to the observations. It is therefore decided not to assume east slope parameters for either case and to calibrate both slopes separately in an endeavor to find better fitting values of α^{-1}, n and K_s.

5.4 Computer model calibration

In total, approximately 1,200 simulations were conducted in CATHY for each hillslope. It appeared that the best 20 simulations of the central slope could be achieved with parameter ranges of α^{-1} = [–0.257 m; –

0.137 m], n = [1.73; 2.09] and K_s = [1.64·10^{-4} m s^{-1}; 1.99·10^{-4} m s^{-1}], yielding a model efficiency coefficient of 0.956 on average. These ranges may also be found in Table 4, as well as the single optimal parameter values. The optimal values as obtained from the soil water retention curve (–0.323 m and 2.22 respectively) are not included in these ranges. This may be explained through the fact that the calibration technique does take the saturated hydraulic conductivity into account whereas the soil water retention curves do not. The former technique yields a higher average model efficiency coefficient of 0.965, suggesting model simulations are of good quality.

Calibration of CATHY to match west slope experiment observations generated optimal ranges of α^{-1} = [–0.573 m; –0.370 m], n = [1.97; 2.60] and K_s = [1.05·10^{-4} m s^{-1}; 1.37·10^{-4} m s^{-1}]. Single optimal values may be reviewed in Table 4. Model performance in this case was slightly worse, averaging at E = 0.941 for the best 20 simulations. This value still reflects strong simulation potential. CATHY's visual output using calibrated input parameters can be found in Figures 15 and 16. Visual calibration output can be found in Appendix D, where variations of the three input parameters and their resulting model efficiency E are depicted.

Table 4: Calibration results comprising optimal ranges and values for α, n and K_s for both hillslopes. The (average) optimal model efficiency coefficient E is included.

	Central range	Central optimal	West range	West optimal
α^{-1} (m)	[–0.257; –0.137]	–0.197	[–0.573; –0.370]	–0.444
n (–)	[1.73; 2.09]	1.88	[1.97; 2.60]	2.25
K_s (10^{-4} m s^{-1})	[1.64; 1.99]	1.79	[1.05; 1.37]	1.19
Average E	**0.956**	**0.965**	**0.930**	**0.941**

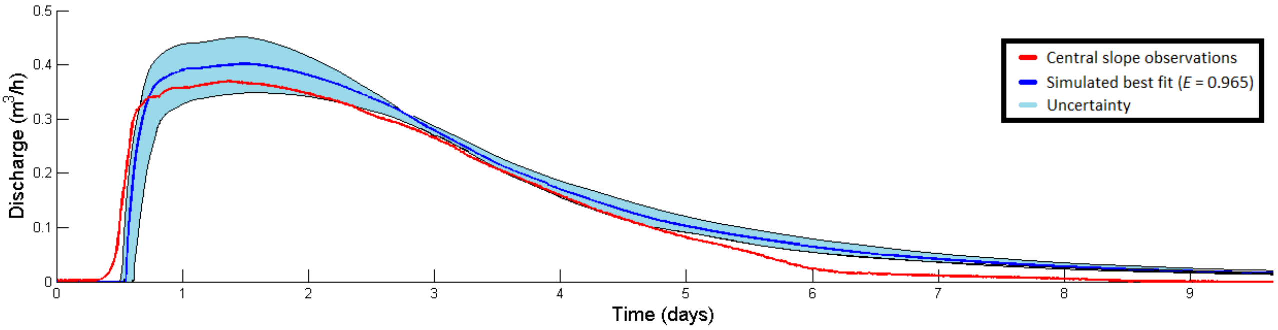

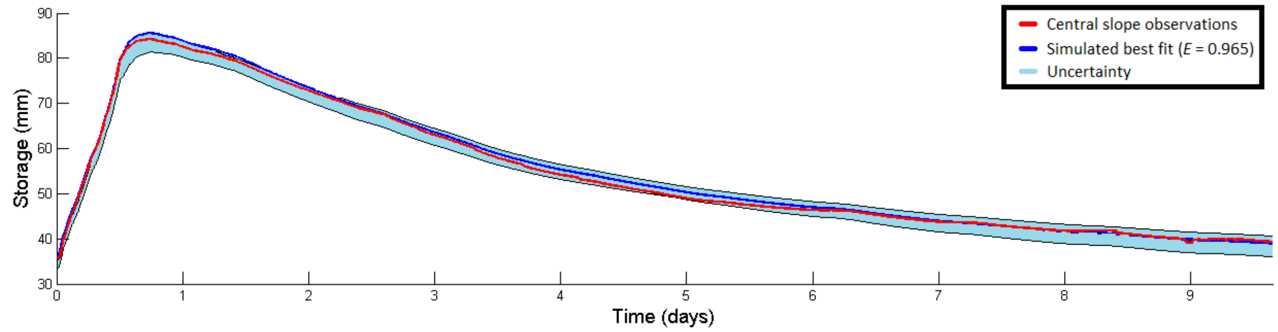

Figure 15: Central slope model output (discharge and storage as functions of time) using optimal input values found using calibration. The red lines represent observed values, the dark blue line the simulated the input values which yield the highest goodness-of-fit coefficient. The light blue bandwidth depicts outcome variety when the optimal ranges are used as input.

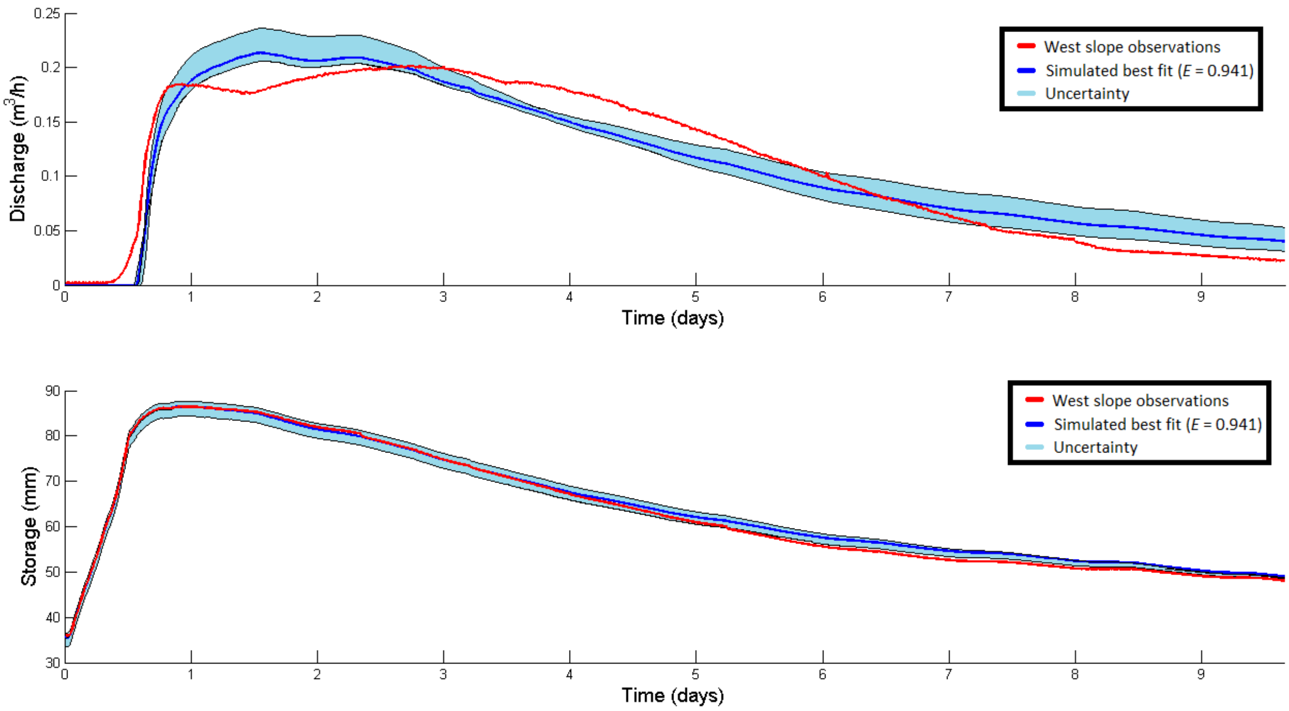

Figure 16: West slope model output (discharge and storage as functions of time) using optimal input values found using calibration. The red lines represent observed values, the dark blue line the simulated the input values which yield the highest goodness-of-fit coefficient. The light blue bandwidth depicts outcome variety when the optimal ranges are used as input.

The calibration results reveal some interesting differences between both hillslopes. Especially the values of α^{-1} show a remarkable distinction; it would seem that the optimal value of α^{-1} in the west slope more than twice the its value in the central slope in absolute terms. Though the pore size distribution index *n* does show some slight differences among the slopes, these cannot be considered very significant. The central slope's soil appears to boast a greater hydraulic conductivity than the west slope's soil, but this difference is marginal in light of the wide array of saturated hydraulic conductivity values which sandy soils may feature (ranging from approximately $2 \cdot 10^{-4}$ m s^{-1} to $3.5 \cdot 10^{-5}$ m s^{-1} (Clapp & Hornberger, 1978; Saxton & Rawls, 2006)).

The model results in terms of discharge and storage as functions of time have been plotted and may be found in Figure 15 and 16. It depicts a staggering improvement over the base runs as visualized in Figure 14, both qualitatively and quantitatively. The used goodness-of-fit coefficients all boast values of at least 0.93, indicating that the model performance is excellent when modeled values are compared to observed values. The simulations of the central and west slopes both show some retardation in incipient discharge flows. In both cases, the model is several hours late simulating increasing discharge flows. These deviations may stem from the model assumption that the soil is completely homogeneous with regard to the saturated hydraulic conductivity. Through this assumption, the model is not able to show much nuance in its discharge rates. This may also be observed as discharge rates start to go up: the modeled series shows a sudden surge upward whereas observed values grow more slowly and look more like an S-curve.

5.5 Underlying causes of found difference

Seeing as mainly the value of α^{-1} seems to show a considerable difference between the central and west hillslopes, we may conclude that the depth of the capillary fringe differs in the slopes. After all, its value is directly related to the depth of the capillary fringe. Using the optimal values of the parameters α^{-1} and n as found through the calibration procedure, the theoretical soil water retention curves of both hillslopes were drawn, to be found in Figure 17.

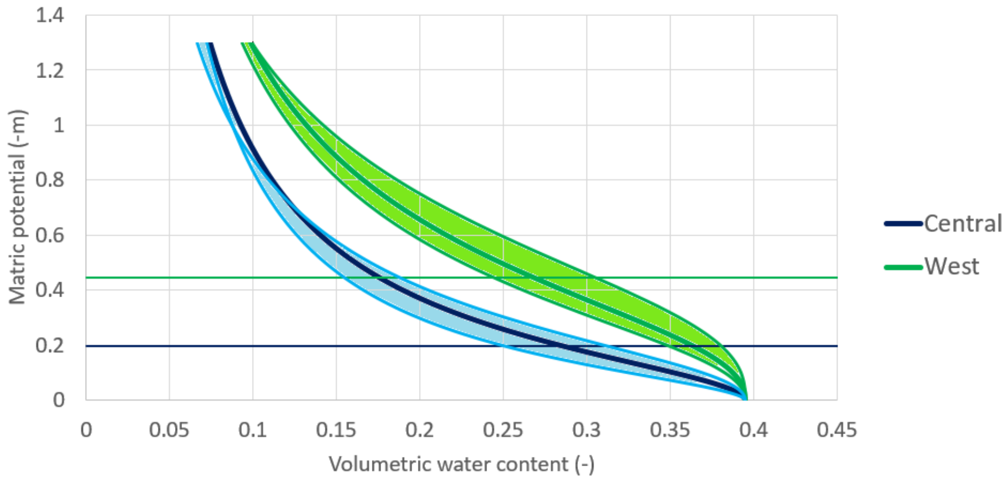

Figure 17: Theoretical soil water retention curve according to the Van Genuchten model assuming optimal values of α^{-1} and n (thick blue respectively green line for the central and west slope) and uncertainty margins according to the found optimal ranges. The horizontal lines indicate the slopes' respective capillary fringe depths. Note that this figure is purely theoretical and does not depict any observations made.

The greater degree of uncertainty in the west slope regarding the two parameters involved is echoed in Figure 17. As may be expected, the lower position of the central slope's curve once more indicates its ability to discharge water faster than the west slope. In line with the other water retention curves presented in this thesis, soil porosity was assumed constant at 0.395 and both curves eventually converge to this point.

Since there did not seem to be a single, logical explanation for the apparent discrepancy in capillary fringe depths, it was decided to share the results reported in the previous sections during a short seminar and discuss them with other LEO research staff. Although no clear-cut possible causes of the difference were raised, the general opinion was that the west slope probably contains more fine soil particles than the central slope. This would explain why the west slope's capillary fringe is located closer to the surface and it discharges water at a lower rate as compared to the central hillslope, despite similar porosity. This is merely the main hypothesis at this point and needs testing, for instance through soil sampling, before it can be accepted or rejected.

6 Discussion

The results of this research and their implications are discussed in this chapter. It is important to acknowledge that methods employed and results found in any research are never optimal or fully representative for the truth. Choices which may affect the research quality have to be made, for example due to temporal, computational or knowledge constraints. These choices naturally influence the outcomes of any research and leave their mark on the conclusions which are drawn. This chapter aims to discuss the choices and assumptions made regarding data analysis (section 6.1) and methodology and CAHTY (section 6.2) which may have had major impact on the results found in this particular research. Finally, section 6.3 briefly discusses the results found in light of past and future research at LEO.

6.1 Data

It is first important to realize that many conclusions drawn from this research are based on just one experiment series. Though experiment series A boasts many parallels in the central and west slope cases and entails a long-lasting experiment, results may differ when other experiment series are examined. Most results obtained during this research seem to be in accordance with each other and explain the difference in observations, but analysis of a greater number of cases may bolster or contradict the conclusions drawn here.

Also, the correction applied to the observed discharge data in the central slope is debatable. Given the circumstances there appeared no obvious alternatives other than correcting the discharge data in the manner described. Without applying any correction, it would not have been possible to determine model performance properly. It is important to bear in mind that the slopes' seepage faces are susceptible to clogging during future experiments. Increased awareness of this issue is necessary to avoid extended episodes of clogging, improving experiment reliability and hopefully eliminating the need to correct any data.

In addition, missing data entries may have had impact on the results found in this research, especially so in the case of the plotted soil water retention curves and probably to a greater extent in the west slope than in the central slope. Since faulty sensors readings are usually clustered in certain hillslope areas, soil moisture and matric potential may not have been properly registered in certain hillslope areas. Though Pasetto et al. (2015) concluded that a minimum of 100 working sensors must be present, they do assume that the sensors working properly are more or less evenly distributed across the hillslope. This issue is being worked on, however, probably allowing for more reliable data in future experiments.

6.2 Methodology and computer model

It is necessary to acknowledge that the results gathered and discussed in this research still rely on some important model idealizations and abstractions, in spite of LEO's controlled environment. While LEO is unique in its field because of this fully controlled environment as was discussed in the state of the art, it does have to deal with some model assumptions. For instance, the Van Genuchten model has been assumed throughout this research. Although often renowned in its field, the Van Genuchten model is highly empirical and features many abstractions and idealizations to simplify the equation. In fact, one of its goals was to reduce the number of parameters involved at the cost of accuracy (van Genuchten, 1980). This has a direct influence on many of the results of this research, which mainly entails comparing the Van Genuchten parameters of both slopes.

Moreover, despite its eminence in the field of hillslope hydrology, CATHY still simplifies many processes and equations to reduce computational costs. For instance, it assumes one Digital Elevation Model (DEM) for all three hillslopes, so it may be universally used to simulate each of them. As stated in subsection

2.1.2, there are minor deviations in the actual soil layer depths as compared with the initial design. CATHY also assumes the Van Genuchten model and homogeneity in soil characteristics across the hillslopes. The great number of assumptions involved may very well have contributed to the clear discrepancy between the Van Genuchten parameters found by means of calibration and those plotted using in-situ measurements.

While CATHY is capable of simulating the rainfall-runoff experiments well, the sole use of CATHY does imply a somewhat biased view in that any errors or uncertainty in the computer model directly propagate to the results. For example, CATHY deliberately ignores any hysteresis observed in soil water retention curves, whereas Figure 5 clearly shows its presence. Using another cutting-edge hydrological model would undoubtedly generate other results and may be complimentary to CATHY.

6.3 Results

Regardless of the issues discussed, this research did shed some more light on why the two slopes differ in terms of soil water characteristics. The observations are mostly clear and resulting optimal input parameters ought to enable LEO scientists to model the central and west slopes accurately during future experiments. It has become indisputable that the slopes differ significantly and LEO researchers are now challenged to test the hypotheses that were put forward in section 5.5 in an attempt to deliver conclusive proof as to the discrepancy that was observed.

Comparing this research to the previous study of LEO's east slope by Niu et al. (2014) one may find many parallels in methodology, usage of models and assumptions. As a result, the optimal parameters of α^{-1}, n and K_s found here are in a similar order of magnitude. Also, the clear difference in soil characteristics justifies the decision to focus solely on these parameters and disregard any other variables which in essence could have been responsible for the observed differences.

This research has also shown that the central and west hillslopes can be simulated in CATHY quite accurately despite the assumption of homogeneity in soil characteristics and thus neglecting any spatial variability in these characteristics. While Niu et al. (2014) did have to modify CATHY and assume a certain degree of heterogeneity in order to obtain accurate simulations of the east slope, such was not necessary in this research. This further strengthens the hypothesis which Niu et al. put forward in 2014, stating that overland flow may have caused incipient heterogeneity in the east slope's soil. After all, no surface flow was observed during central and west slope experiments. What is more, the excellent model performance implies that the soil in the central and west slopes is still more or less homogeneous.

7 Conclusions and recommendations

This chapter treats the conclusions reached at the end of this research project as well as some suggestions for further research at LEO grounds. The answers to the various research questions were formulated in the partial conclusions described throughout chapter 5. Section 7.1 uses them to refer back to the original research aim and close the research gap described in section 1.3. Some recommendations for further research are subsequently made in section 7.2.

7.1 Conclusions

From the analysis of the S,t and Q,t plots it has become clear that there is a significant discrepancy in terms of water transit times between the central and west hillslopes. Because the central slope discharges water at a higher rate – at some points in time even twice the rate of the west slope – it loses water faster. This is reflected by the sharper decline of total water storage over time, as depicted in the S,t plots. The found variation in the important soil parameters α^{-1} and n from in-situ measurements underlines this difference and has been an important indication in further research steps. Considering that the observed differences in discharge-over-time, storage-over-time and soil parameters are substantial (exceeding a factor of 1.5 in some cases, such as the maximum discharge observed), the conclusion may be drawn that the two hillslopes indeed differ significantly in terms of water retention times and that variation in soil water characteristics are likely to play some role in this discrepancy.

This hypothesis is supported by CATHY model simulations, optimizing for the model efficiency coefficient. It shows that the central hillslope can best be simulated using values of α^{-1} of about –0.20 m, whereas a value around –0.45 m seems to be optimal in the west slope. This difference, which represents differing depths of the slopes' capillary fringes, is very significant. While slight variations in optimal values of n and K_s were also found, these are considered to be minor. Therefore the main conclusion drawn is that the central and west slopes feature different soil water characteristics in terms of the depth of their capillary fringe.

It was not possible to find a precise cause of the difference in capillary fringe between the slopes in the context of this research. However, some hypotheses were formulated which may be tested in future research projects seeking to further address the question of differing hillslopes. At this point the author of this thesis chooses to embrace the theory that the west slope's soil contains more fine particles than the central slope, explaining the found difference in capillary fringe and enhanced water retention characteristics.

Finally, another important conclusion based on this research – albeit beyond its aim and scope – is that the central slope bears less resemblance with the east slope than was presumed in the past. This finding, based on CATHY simulations of central and west slope cases under east slope optimum input, contradicts the hypothesis that LEO scientists have proposed.

7.2 Recommendations

One of the main recommendations following this report's results and conclusions would be to sample the central and west slopes' soils to test the hypothesis that the west slope's soil contains more fine particles. Acceptance of that hypothesis could deliver more conclusive proof with regard to the discrepancy between both slopes.

Also, it is recommended that more simultaneous experiments be conducted and their results be analyzed. Carrying out rainfall-runoff experiments on the three slopes simultaneously would be an important step in further increasing experiment accuracy. Analysis in a similar manner as employed in this research of other and new experiments is deemed necessary to confirm and reinforce conclusions drawn in this research and improve general credibility of the LEO project. For instance, optimal model configuration as found in this research may be used to simulate other and newly conducted experiments to see whether model predictions are in accordance with new and other observations. In fact, observations may change as the slopes have been through more wetting and drying cycles as a result of incipient landscape changes through rainfall-runoff experiments.

References

Andersen, J., Refsgaard, J. C., & Jensen, K. H. (2001). Distributed hydrological modelling of the Senegal River Basin - Model construction and validation. *Journal of Hydrology*, *247*(3-4), 200–214. http://doi.org/10.1016/S0022-1694(01)00384-5

ASCE. (1993). Criteria for Evaluation of Watershed Models. *Journal of Irrigation and Drainage Engineering*, *119*(3), 429–442.

Bogena, H., Borg, E., Brauer, A., Dietrich, P., Hajnsek, I., Heinrich, I., … Zacharias, S. (2016). TERENO: German network of terrestrial environmental observatories. *Journal of Large-Scale Research Facilities*, *52*, 1–8. http://doi.org/http://dx.doi.org/10.17815/jlsrf-2-98

Brooks, R. H., & Corey, A. T. (1964). Hydraulic properties of porous media. *Hydrology Papers Colorado State University*, *3*(3), 1–27.

Camporese, M., Paniconi, C., Putti, M., & Orlandini, S. (2010). Surface-subsurface flow modeling with path-based runoff routing, boundary condition-based coupling, and assimilation of multisource observation data. *Water Resources Research*, *46*, W02512. http://doi.org/10.1029/2008WR007536

Clapp, R. B., & Hornberger, G. M. (1978). Empirical Equations for Some Soil Hydraulic Properties. *Water Resources Research*, *14*(4), 601–604.

Clarke, R. T. (1973). A review of some mathematical models used in hydrology, with observations on their calibration and use. *Journal of Hydrology*, *19*(1), 1–20. http://doi.org/10.1016/0022-1694(73)90089-9

Criss, R. E., & Winston, W. E. (2008). Do Nash values have value? Discussion and alternate proposals. *Hydrological Processes*, *22*(14), 2723–2725. http://doi.org/10.1002/hyp.7072

Dezetter, A., & Servat, E. (1991). Selection of calibration objective functions in the context of rainfall-runoff modelling in a sudanese savannah area. *Hydrological Sciences - Journal - Des Sciences Hydrologiques*, *36*(4), 307–330. http://doi.org/10.1080/02626669109492517

Dontsova, K., Steefel, C. I., Desilets, S., Thompson, A., & Chorover, J. (2009). Coupled modeling of hydrologic and geochemical fluxes for prediction of solid phase evolution in the Biosphere 2 hillslope experiment. *Hydrology and Earth System Sciences Discussions*, *6*, 4449–4483. http://doi.org/10.5194/hessd-6-4449-2009

Eberhardt, L. L., & Thomas, J. M. (1991). Designing Environmental Field Studies. *Ecological Monographs*, *61*(1), 53–73.

Gerwin, W., Raab, T., Biemelt, D., Bens, O., & Hüttl, R. F. (2009). The artificial water catchment "Chicken Creek" as an observatory for critical zone processes and structures. *Hydrology and Earth System Sciences Discussions*, *6*(2), 1769–1795. http://doi.org/10.5194/hessd-6-1769-2009

Gevaert, A. I., Teuling, A. J., Uijlenhoet, R., DeLong, S. B., Huxman, T. E., Pangle, L. A., … Troch, P. A. (2014). Hillslope-scale experiment demonstrates the role of convergence during two-step saturation. *Hydrology and Earth System Sciences*, *18*(9), 3681–3692. http://doi.org/10.5194/hess-18-3681-2014

Graham, D. N., & Butts, M. B. (2005). Flexible Integrated Watershed Modeling with MIKE SHE. In V. P. Singh & D. K. Frevert (Eds.), *Watershed Models* (pp. 245–272). Boca Raton, FL: CRC Press.

Gupta, H. V., Kling, H., Yilmaz, K. K., & Martinez, G. F. (2009). Decomposition of the mean squared error and NSE performance criteria: Implications for improving hydrological modelling. *Journal of Hydrology*, *377*(1-2), 80–91. http://doi.org/10.1016/j.jhydrol.2009.08.003

Hazenberg, P., Broxton, P., Gochis, D., Niu, G.-Y., Pangle, L. A., Pelletier, J. D., … Zeng, X. (2016). Testing the hybrid-3-D hillslope hydrological model in a controlled environment. *Water Resources Research*, *52*(2), 1089–1107. http://doi.org/10.1002/2015WR018106

Hernandez, C. M., & Schaap, M. G.: Hydrology simulations on basalt soil for the Landscape Evolution Observatory (LEO), Abstract No. H53I-1644, AGU Fall Meeting, 3–7 December 2012, San Francisco, 2012.

Hofer, M., Lehmann, P., Biemelt, D., Stähli, M., & Krafczyk, M. (2011). Modelling subsurface drainage pathways in an artificial catchment. *Physics and Chemistry of the Earth*, *36*(1-4), 101–112. http://doi.org/10.1016/j.pce.2010.04.020

Hopp, L., Harman, C., Desilets, S. L. E., Graham, C. B., Mcdonnell, J. J., & Troch, P. A. (2009). Hillslope hydrology under glass: confronting fundamental questions of soil-water-biota co-evolution at Biosphere 2. *Hydrology and Earth System Sciences*, *13*, 2105–2118.

Huxman, T., Troch, P., Chorover, J., Breshears, D. D., Saleska, S., Pelletier, J., … Espeleta, J. (2009). The hills are alive: Earth science in a controlled environment. *Eos*, *90*(14), 120. http://doi.org/10.1029/2009EO140003

Huyakorn, P. S., Thomas, S. D. and Thompson, B. M. (1984), Techniques for making finite elements competitive in modeling flow in variably saturated porous media, *Water Resources Research, 20(8)*, 1099–1115.

Kampf, S. K., & Burges, S. J. (2007). A framework for classifying and comparing distributed hillslope and catchment hydrologic models. *Water Resources Research*, *43*(5). http://doi.org/10.1029/2006WR005370
Krause, P., Boyle, D. P., & Bäse, F. (2005). Comparison of different efficiency criteria for hydrological model assessment. *Advances In Geosciences*, *5*(89), 89–97. http://doi.org/10.5194/adgeo-5-89-2005
Ley, R., Hellebrand, H., Casper, M. C., & Fenicia, F. (2015). Comparing classical performance measures with signature indices derived from flow duration curves to assess model structures as tools for catchment classification. *Hydrology Research, 47*(3), 1-15. http://doi.org/10.2166/nh.2015.221
Lin, H., Bouma, J., Pachepsky, Y., Western, A., Thompson, J., & Genuchten, R. Van. (2006). Hydropedology: Synergistic integration of pedology and hydrology. *Water Resources Research*, *42*, 1–13. http://doi.org/10.1029/2005WR004085
Loague, K., & Vanderkwaak, J. E. (2002). Simulating hydrological response for the R-5 catchment: Comparison of two models and the impact of the roads. *Hydrological Processes*, *16*(5), 1015–1032. http://doi.org/10.1002/hyp.316
McCuen, R. H., Knight, Z., & Cutter, A. G. (2006). Evaluation of the Nash–Sutcliffe Efficiency Index. *Journal of Hydrologic Engineering*, *11*(6), 597–602. http://doi.org/10.1061/(ASCE)1084-0699(2006)11:6(597)
McDonnell, J. J., Sivapalan, M., Vache, K., Dunn, S., Grant, G., & Haggerty, R. (2007). Moving beyond heterogeneity and process complexity: A new vision for watershed hydrology. *Water Resources Research*, *43*, 1–6. http://doi.org/10.1029/2006WR005467
Mualem, Y. (1976). A New Model for Predicting the Hydraulic Conductivity of Unsaturated Porous Media. *Water Resources Research*, *12*(3), 513–522.
Nash, J. E., & Sutcliffe, J. V. (1970). River Flow Forecasting Through Conceptual Models Part I-a Discussion of Principles. *Journal of Hydrology*, *10*, 282–290. http://doi.org/10.1016/0022-1694(70)90255-6
Niu, G. Y., Pasetto, D., Scudeler, C., Paniconi, C., Putti, M., Troch, P. A., … Zeng, X. (2014). Incipient subsurface heterogeneity and its effect on overland flow generation - Insight from a modeling study of the first experiment at the Biosphere 2 Landscape Evolution Observatory. *Hydrology and Earth System Sciences*, *18*(5), 1873–1883. http://doi.org/10.5194/hess-18-1873-2014
Pangle, L. A., DeLong, S. B., Abramson, N., Adams, J., Barron-Gafford, G. A., Breshears, D. D., … Zeng, X. (2015). The Landscape Evolution Observatory: A large-scale controllable infrastructure to study coupled Earth-surface processes. *Geomorphology*, *244*, 190–203. http://doi.org/10.1016/j.geomorph.2015.01.020
Paniconi, C., & Putti, M. (1994), A comparison of Picard and Newton iteration in the numerical solution of multidimensional variably saturated flow problems, *Water Resources Research*, *30(12)*, 3357–3374.
Paniconi, C., & Wood, E. F. (1993). A Detailed Model for Simulation of Catchment Scale Subsurface Hydrologic Processes. *Water Resources Research*, *29*(6), 1601–1620.
Pasetto, D., Niu, G. Y., Pangle, L., Paniconi, C., Putti, M., & Troch, P. A. (2015). Impact of sensor failure on the observability of flow dynamics at the Biosphere 2 LEO hillslopes. *Advances in Water Resources*, *86*, 327–339. http://doi.org/10.1016/j.advwatres.2015.04.014
Richards, L. A. (1931). Capillary conduction of liquids through porous mediums. *Journal of Applied Physics*, *1*(5), 318–333. http://doi.org/10.1063/1.1745010
Ritzema, H. P. (2006). *Drainage Principles and Applications* (16th ed.). Wageningen: Alterra-ILRI.
Saxton, K., & Rawls, W. (2006). Soil Water Characteristic Estimates by Texture and Organic Matter for Hydrologic Solutions. *Soil Science Society of America Journal*, *70*, 1569–1578. http://doi.org/10.2136/sssaj2005.0117
Scudeler, C., Pangle, L., Pasetto, D., Niu, G.-Y., Volkmann, T., Paniconi, C., … Troch, P. (2016). Multiresponse modeling of an unsaturated zone isotope tracer experiment at the Landscape Evolution Observatory. *Hydrology and Earth System Sciences Discussions*, (May), 1–29. http://doi.org/10.5194/hess-2016-228
Seager, R., Ting, M., Held, I., Kushnir, Y., Lu, J., Vecchi, G., … Naik, N. (2007). Model Projections of an Imminent Transition to a More Arid Climate in Southwestern North America. *Science*, *316*(5828), 1181–1184. http://doi.org/10.1126/science.1139601
Singh, V., & Bhallamudi, S. M. (1998). Conjunctive surface-subsurface modeling of overland flow. *Advances in Water Resources*, *21*(7), 567–579. http://doi.org/10.1016/S0309-1708(97)00020-1
Smith, P., Beven, K. J., & Tawn, J. A. (2008). Informal likelihood measures in model assessment: Theoretic development and investigation. *Advances in Water Resources*, *31*(8), 1087–1100. http://doi.org/10.1016/j.advwatres.2008.04.012
Stephenson, G. R., & Freeze, R. A. (1974), Mathematical simulation of subsurface flow contributions to snowmelt runoff, Reynolds Creek Watershed, Idaho, *Water Resources Research, 10(2), 284–294*
Todini, E. (1988). Rainfall-runoff modeling - Past, present and future. *Journal of Hydrology*, *100*(1-3), 341–352. http://doi.org/10.1016/0022-1694(88)90191-6

Tuller, M., & Or, D. (2004). Retention of water in soil and the soil water characteristic curve. *Encyclopedia of Soils in the Environment*, *4*, 278–289. Retrieved from http://www.engr.uconn.edu/environ/envphys/pdf/vadose_pdf/SWC_revised01.pdf

van Genuchten, M. T. (1980). A Closed-form Equation for Predicting the Hydraulic Conductivity of Unsaturated Soils. *Soil Science Society of America Journal*, *44*(5), 892–898. http://doi.org/10.2136/sssaj1980.03615995004400050002x

Van Genuchten, M. T., & Nielsen, D. R. (1985). On describing and predicting the hydraulic properties of unsaturated soils. *Annales Geophysicae*, *3*(5), 615–628. http://doi.org/10.1111/j.1468-2494.2010.00560.x

Wagener, T., Sivapalan, M., Troch, P., & Woods, R. (2007). Catchment Classification and Hydrologic Similarity. *Geography Compass*, *1*, 1–31. http://doi.org/10.1111/j.1749-8198.2007.00039.x

Zacharias, S., Bogena, H., Samaniego, L., Mauder, M., Fuß, R., Pütz, T., … Vereecken, H. (2011). A Network of Terrestrial Environmental Observatories in Germany. *Vadose Zone Journal*, *10*(3), 955. http://doi.org/10.2136/vzj2010.0139

Appendix A: experimental set-up

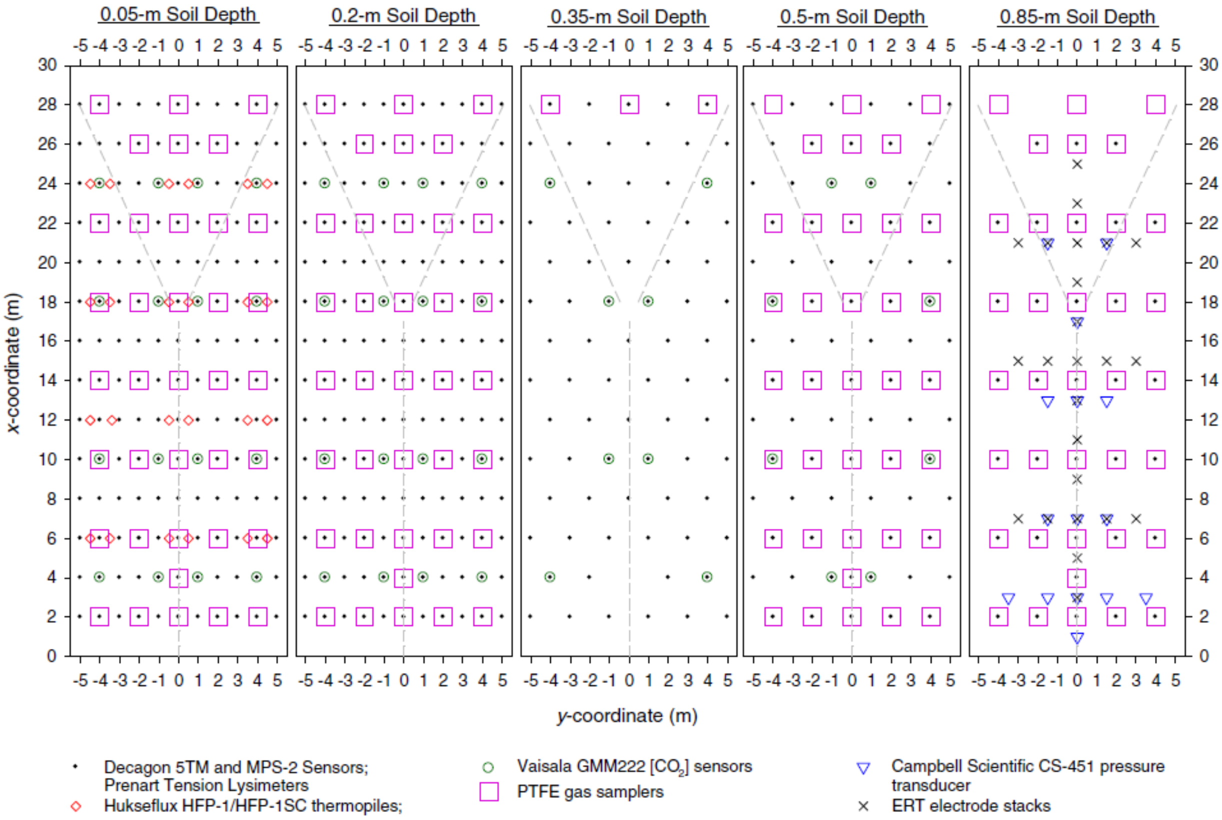

Figure A1: Overview of sensor placements throughout each hillslope. Adapted from ''The Landscape Evolution Observatory: A large-scale controllable infrastructure to study coupled Earth-surface processes'' by L.A. Pangle et al., 2015, Geomorphology, p. 197.

Figure A2: Close-up of a slope's seepage face from above (left) and below (right). The six equally sized outflow zones are well visible. Reprinted from ''The Landscape Evolution Observatory: A large-scale controllable infrastructure to study coupled Earth-surface processes'' by L.A. Pangle et al., 2015, Geomorphology, p. 200.

Appendix B: Additional S,t and Q,t plots

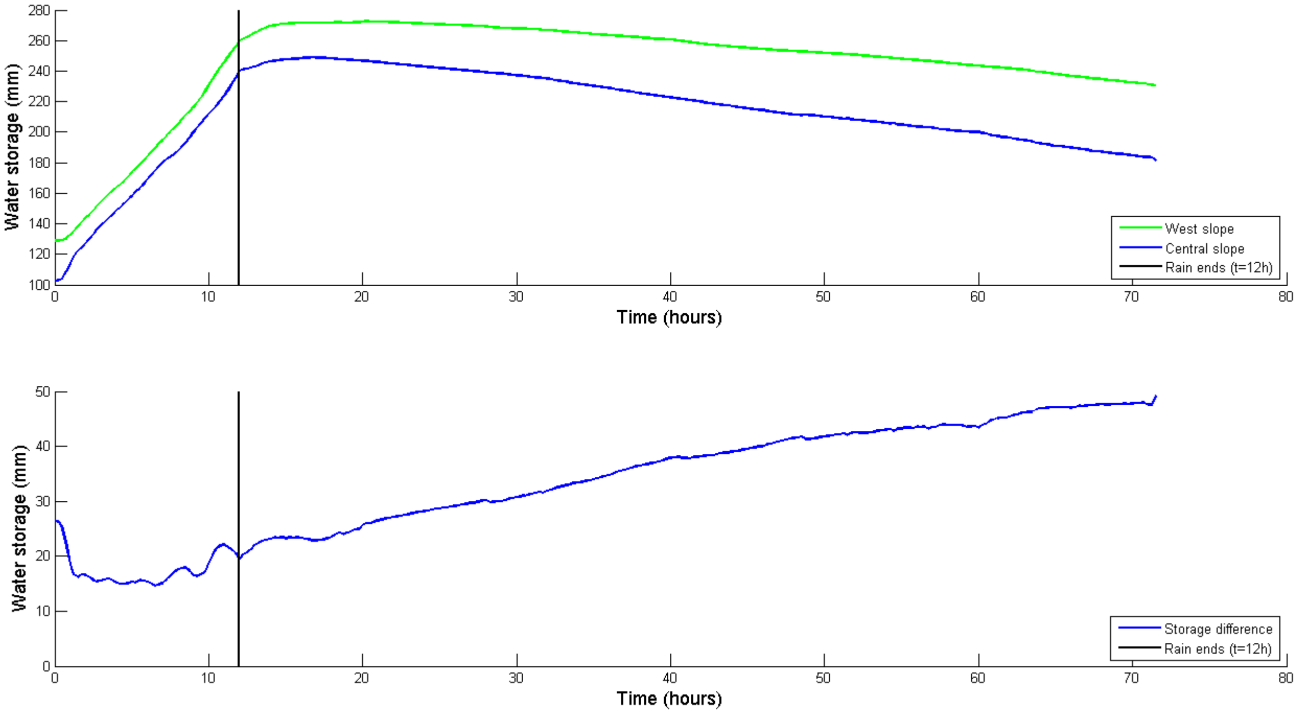

Figure B1 (upper): S,t plot of the central and west hillslopes with data from experiments series B. (lower): The difference of water storage in both slopes over time.

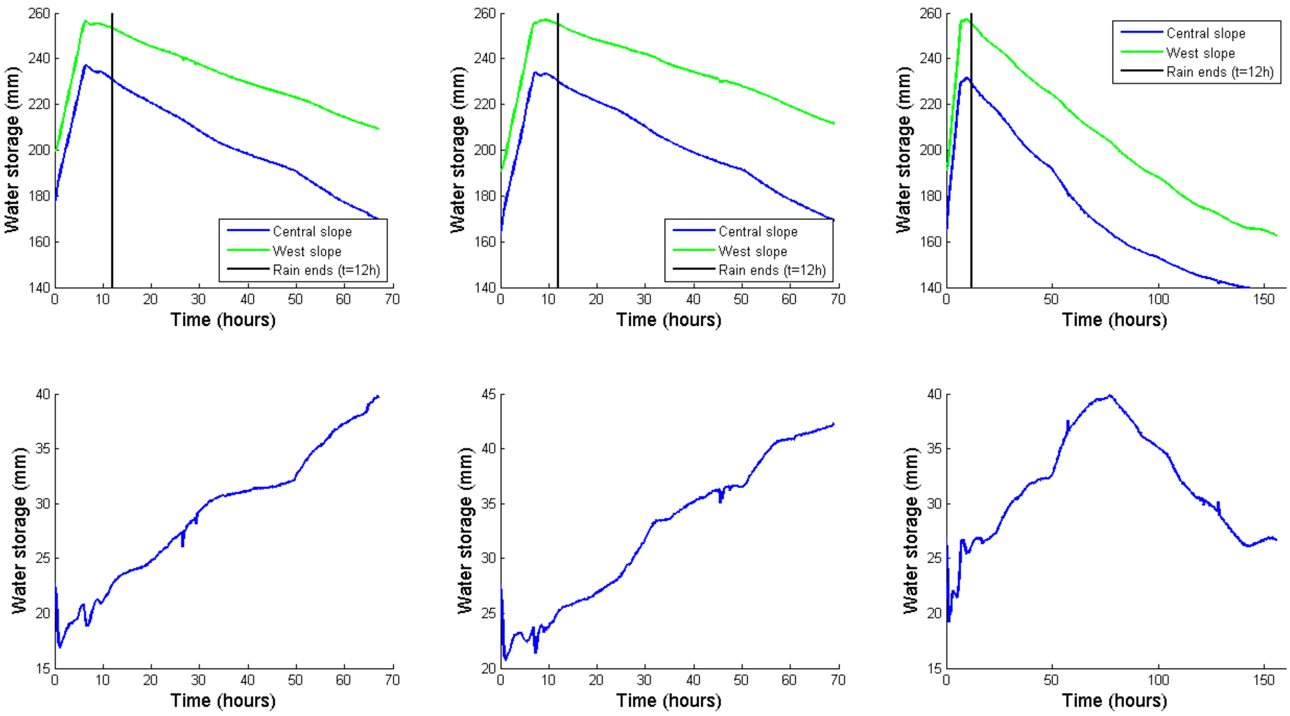

Figure B2: (upper): S,t plots of the central and west hillslopes with data from experiments series C, D and E. (lower): The difference of water storage in both slopes (west minus central) over time. Note that experiment E has a longer time frame than series C and D and its results are presented here accordingly.

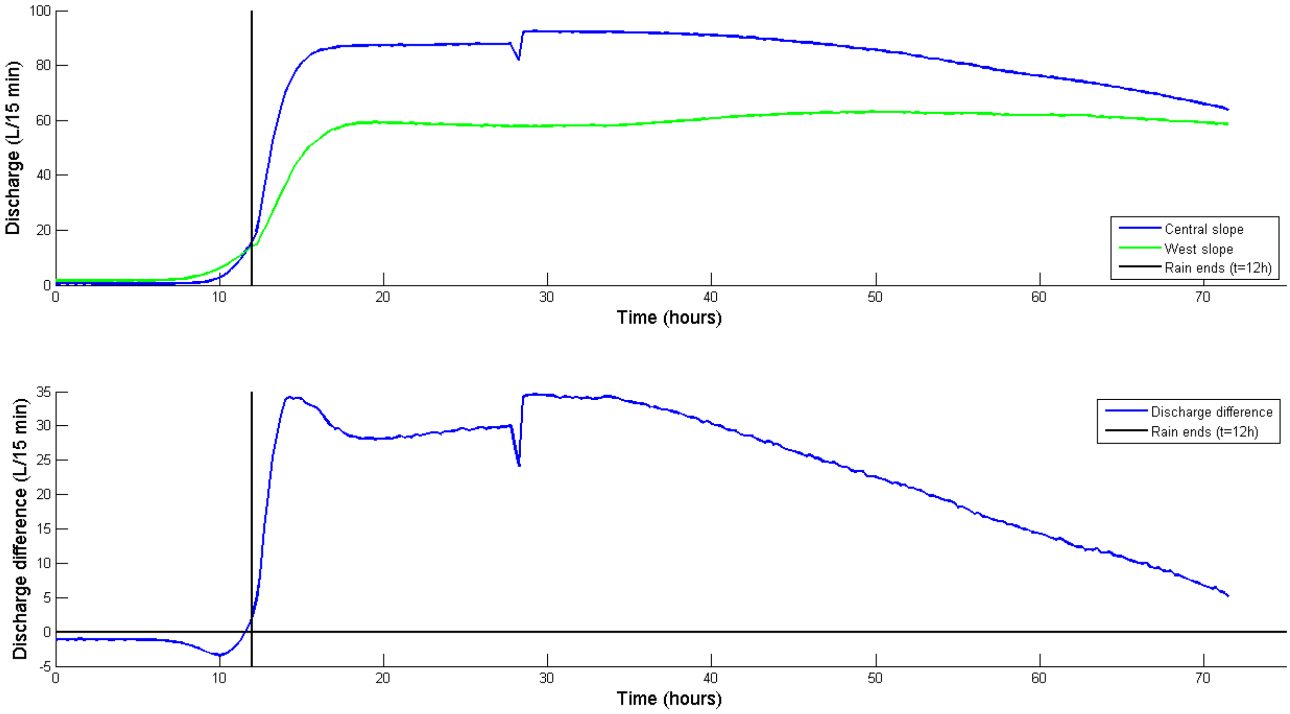

Figure B3 (upper): Q,t plot of the central and west hillslopes with data from experiments series B. (lower): The difference of discharge rates in both slopes over time (central slope discharge minus west slope discharge)

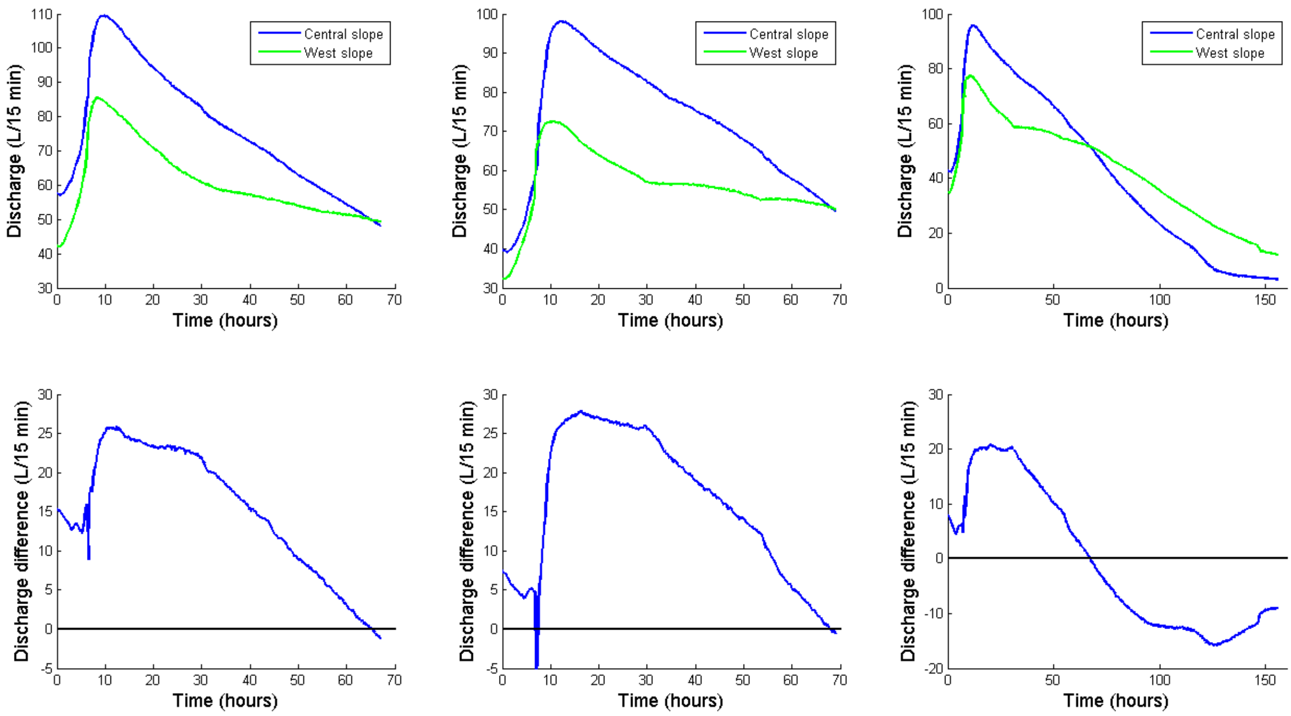

Figure B4: (upper): Q,t plot of the central and west hillslopes with data from experiments series C through E. (lower): The difference of discharge rates in both slopes over time (central slope discharge minus west slope discharge). Note that experiment E has a longer time frame than series C and D and its results are presented here accordingly.

Appendix C: Additional soil water retention curves

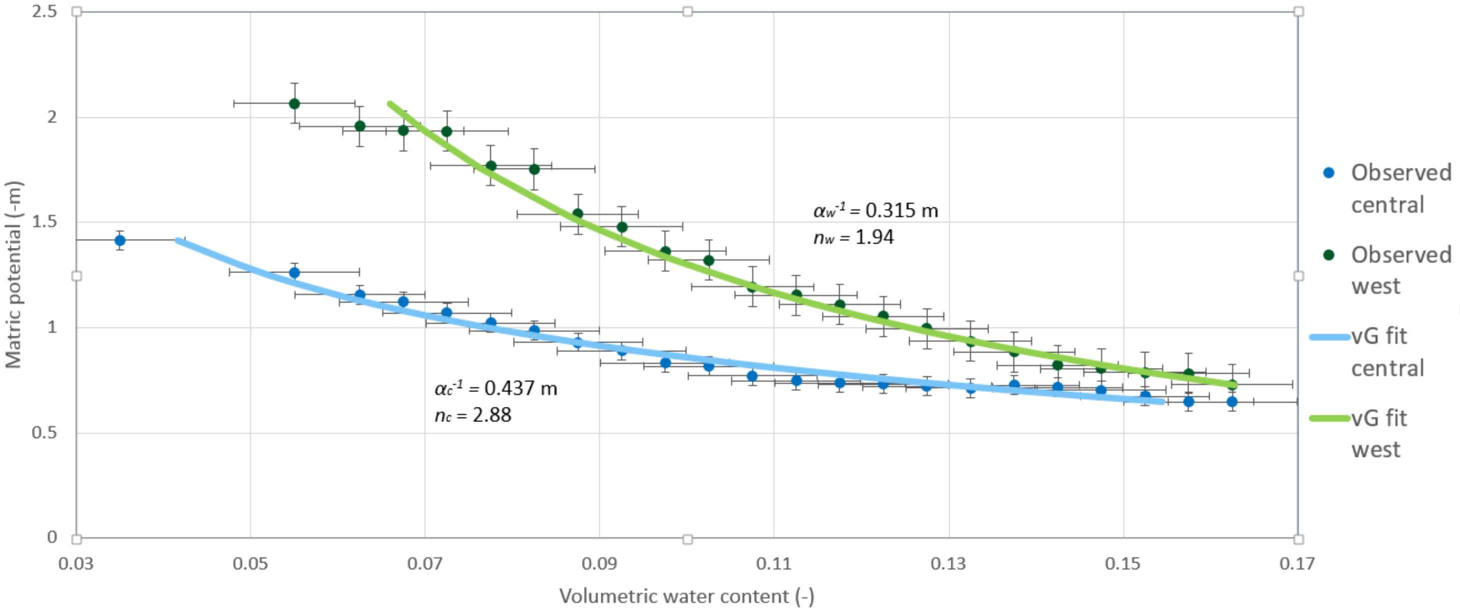

Figure C1: Soil water retention curves using every reliable sensor location in both slopes. Error bars indicating the standard deviation in volumetric water content and matric potential are included. The Van Genuchten model has been fitted to the observations and the resulting values of the fitting parameters α^{-1} and n are included.

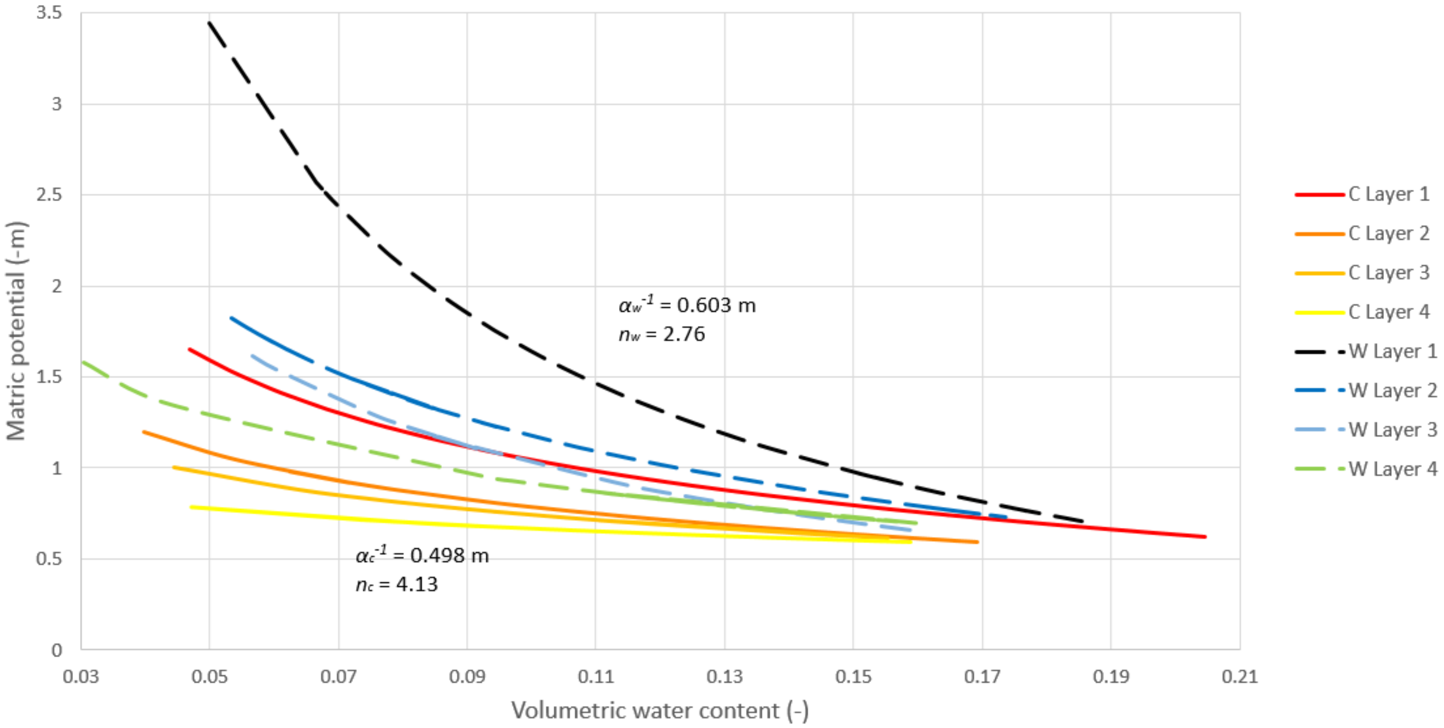

Figure C2: Soil water retention curves plotted per soil layer in both slopes (layer 1 being the topmost layer and layer 4 the bottommost). No reliable of layer 5 was available because of saturated conditions. Only the Van Genuchten model fits and the average values of the fitting parameters are included; observations omitted for clarity.

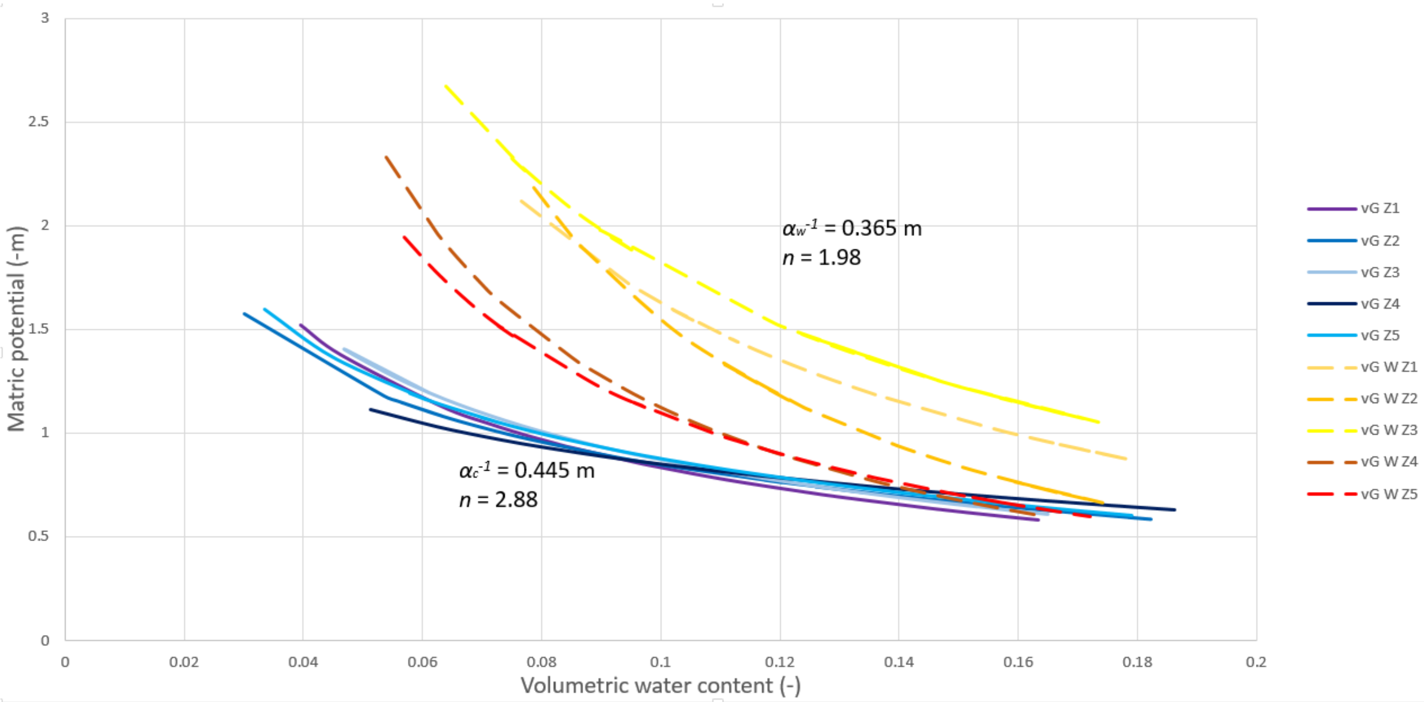

Figure C3: Soil water retention curves plotted per soil zone in both slopes. Exact zone locations may be reviewed in Figure 5. Only the Van Genuchten model fits and the average values of the fitting parameters are included; observations omitted for clarity.

Appendix D: Model calibration

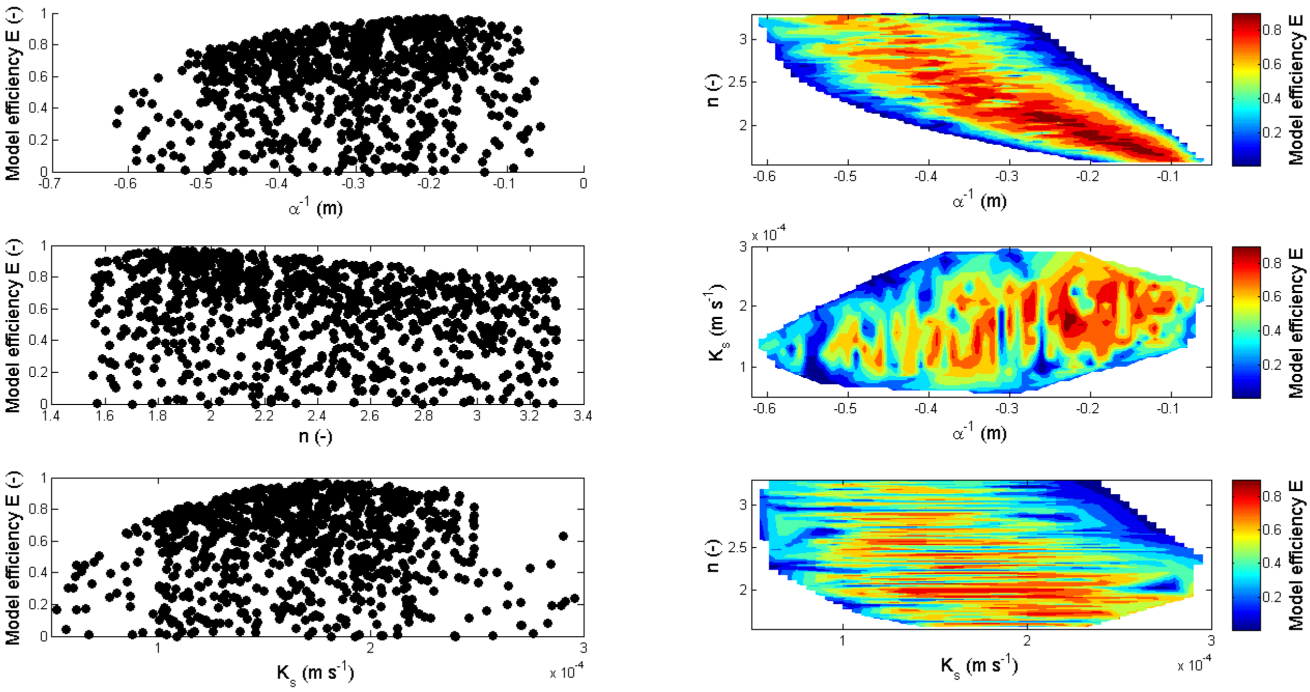

Figure D1 (left): Central slope dotty plots depicting the model efficiency coefficient *E* for variations of each parameter (α^{-1}, *n* and K_s). (Right): Contour plots depicting the model efficiency coefficient *E* (color) for variations of two parameters (α^{-1}/n; α^{-1}/K_s; K_s/n). Note that only positive values of *E* are included; negatives are disregarded.

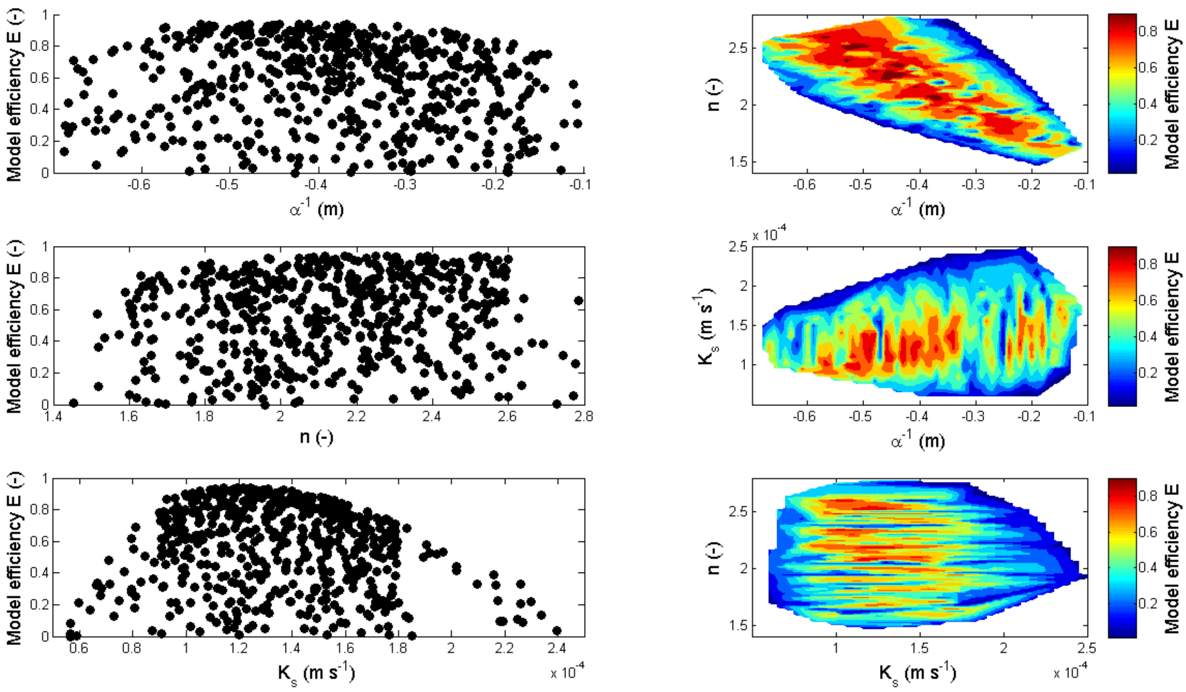

Figure D2 (left): West slope dotty plots depicting the model efficiency coefficient *E* for variations of each parameter (α^{-1}, *n* and K_s). (Right): Contour plots depicting the model efficiency coefficient *E* (color) for variations of two parameters (α^{-1}/n; α^{-1}/K_s; K_s/n). Note that only positive values of *E* are included; negatives are disregarded.